Journal of Nanobiotechnology

RESEARCH

Open Access

Streptococcus mutans-derived extracellular vesicles promote skin wound healing via tRNA cargo

Su Young Oh[1†], Dong Yeon Kim[1†], Kah Young Lee[1], Dae-Lyong Ha[2], Tae-Lyn Kim[1], Tae-Geon Kwon[3], Jin-Wook Kim[3], Heon-Jin Lee[1*], So-Young Choi[3*] and Su-Hyung Hong[1*]

Abstract

Background The human oral cavity harbors a diverse microbiota, including Streptococcus species. Oral mucosal wounds heal rapidly, although the exact cause remains unclear. This study investigates the impact of *Streptococcus mutans*-derived extracellular vesicles (Sm EVs) on wound healing in both oral mucosal organoids and mouse skin. To explore whether microbial EV RNA cargo influences wound healing, RNA sequences from Sm EVs were identified, and the most abundant sequences were synthesized into oligomers and encapsulated in *E. coli* EVs (Ec EVs) for further *in vivo* testing. We assessed the role of Toll-like receptor 3 (TLR3) in the wound healing mechanism in TLR3 knockout (KO) mice.

Results Sm EVs significantly enhanced cell proliferation and migration in oral mucosa, with enhanced focal adhesion complex formation. Sm EVs improved wound healing in mouse dorsal skin compared to PBS controls. RNA sequencing revealed that bacterial tRNAs, particularly the tRNA-Met variant (Oligo 1), were the most abundant RNAs in Sm EVs. Ec EVs carrying Oligo 1 produced similar wound healing effects to Sm EVs in mucosal organoids and mouse dorsal skin. However, in TLR3 knockout mice, Oligo 1 did not improve wound healing.

Conclusions This study highlights the role of Sm EVs, particularly their tRNA variants, in promoting skin wound healing through a TLR3-dependent mechanism. These findings suggest that EVs from oral commensal bacteria may offer therapeutic potential for chronic, non-healing skin wounds.

Keywords *Streptococcus mutans*, Extracellular vesicles, Oral mucosa, Skin wound healing, TLR3, Bacterial tRNA

†Su Young Oh and Dong Yeon Kim contributed equally to this work.

*Correspondence:
Heon-Jin Lee
heonlee@knu.ac.kr
So-Young Choi
dentalchoi@knu.ac.kr
Su-Hyung Hong
hongsu@knu.ac.kr

Full list of author information is available at the end of the article

Graphical Abstract

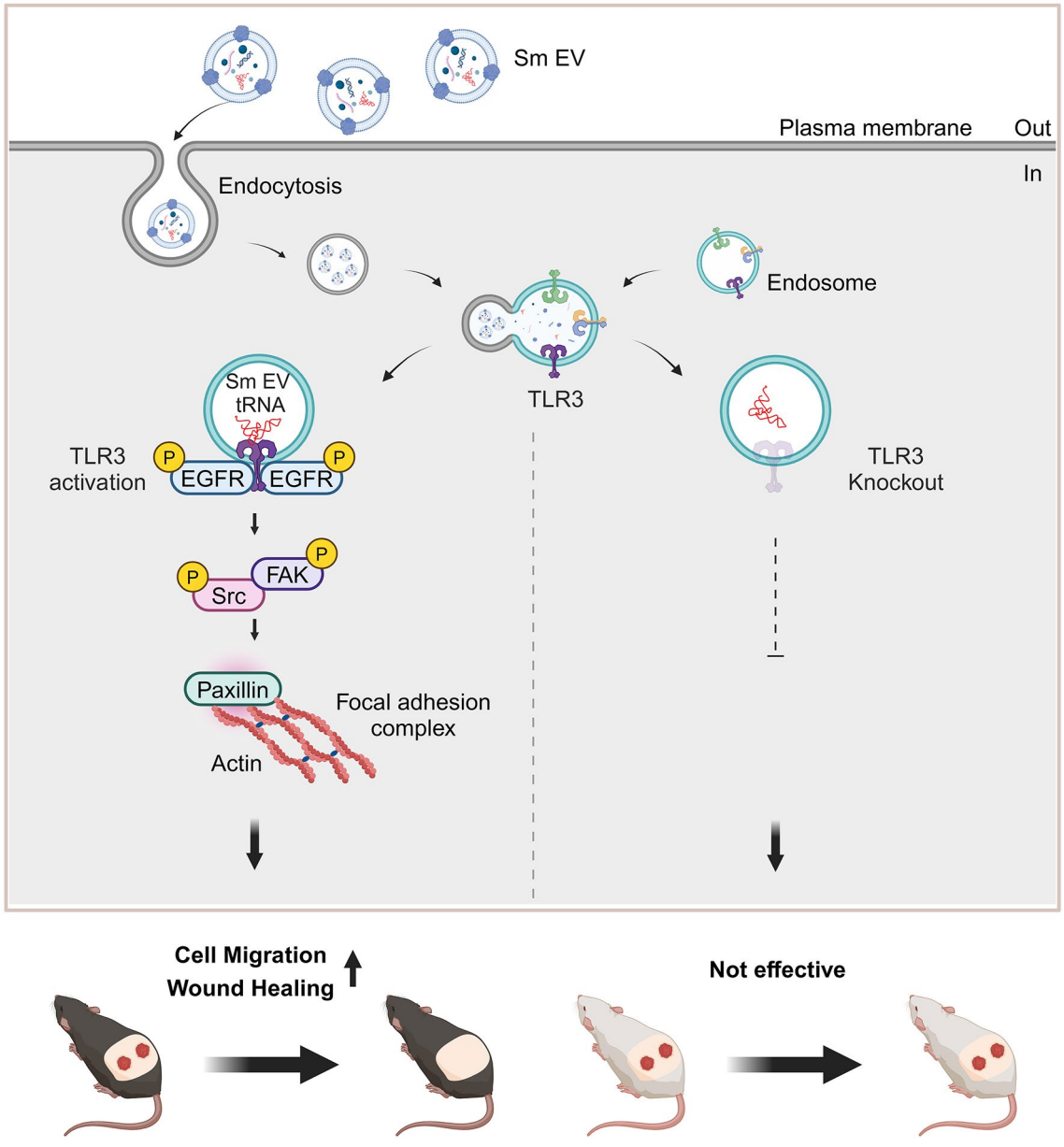

Background

The oral cavity harbors a vast community of commensal bacteria that coexist with the host; although the exact number at any given moment is difficult to pinpoint. It is estimated that the average adult's mouth contains approximately 50–100 billion bacteria representing around 200 dominant bacterial species, most of which are harmless [1–3]. Recent studies revealed that extracellular vesicles (EVs) presenting in the oral environment are key molecules that mediate interactions between the host and microbiota [4]. *Streptococcus mutans*, a Gram-positive bacterium, is one of the predominant microorganisms in the human oral cavity. *S. mutans* is recognized as a primary contributor to dental caries, playing a pivotal role in forming dental biofilms. Both the skin and oral mucosa serve as the body's first line of defense, maintaining homeostasis and protecting against external disruptions. Hence, wound healing in these tissues is a complex, well-orchestrated process involving various cellular and molecular interactions. Traditionally, research has focused on immune cells, growth factors, and extracellular matrix components, but recently, studies have highlighted the role of commensal bacteria in modulating wound healing responses. These bacteria, which inhabit

diverse niches in the body, form mutualistic relationships with their host, influencing infection prevention and tissue repar, particularly in skin and mucosal wounds [5, 6]. For example, certain microbes positively affect skin wound healing by priming the immune system and influencing the wound healing cascade [7–10]. Previous studies demonstrated that oral Streptococci enhanced the wound healing process in a 24 h *in vitro* oral mucosa coculture model [11]. While it has been shown that the lipid component of lipoteichoic acid from *S. mutans* promotes immune stimulation via TLR2 [12], no reports currently link bacterial EVs to mucosal wound healing.

The human oral mucosa is known for its high regenerative capacity, exhibiting rapid wound healing rates that are not significantly influenced by factors including age or gender [13–15]. Despite constant exposure to mechanical stress and various microbes, wounds in the oral mucosa heal quickly with minimal scarring [16]. The basis for this unique healing and regeneration depends on cellular and non-cellular factors. Indeed, Waasdorp et al. suggested faster wound closure and reduced scarring in the oral mucosa, compared to the skin, resulting from factors such as saliva presence, quicker immune response, and enhanced extracellular matrix remodeling [16]. Saliva, in particular, plays a key role in creating a humid environment conducive to the survival and function of inflammatory cells [17]. Moreover, saliva contains several growth factors, which play a significant role in the different stages of wound healing [18, 19]. Furthermore, oral mucosal stem cells secrete additional growth factors [20], which promote cell migration and proliferation, both essential for tissue repair in various physiological and pathological contexts. Additionally, Michalczyk et al. identified changes in the microbiome during oral wound healing, emphasizing the need for novel probiotic delivery methods for oral wounds [21]. However, the precise reasons for the particularly rapid recovery of oral mucosa remain unclear, and little is known about the role of commensal streptococci in this process.

Recently, microbial communication and the exchange of bioactive molecules between commensal bacteria and their host have gained attention, with EVs emerging as crucial mediators of intercellular communication [22, 23]. Bacterial EVs are nano-sized membrane-bound structures released by Gram-positive and Gram-negative bacteria that carry proteins, lipids, and nucleic acids as cargo [24, 25]. *S. mutans*-derived EVs (Sm EVs) are particularly interesting, contributing to the complexity of oral microbial interactions [26]. Sm EVs have previously been implicated in the processes such as biofilm formation [27], host-pathogen interactions [28], and modulation of the host immune response [29]. Therefore, understanding the role of Sm EVs could provide insight into the mechanisms behind the pathogenicity of this bacterium and its broader impact on oral health.

Microbial-derived RNA has also gathered interest as a pathogen-associated molecular pattern (PAMP) that modulates host immune responses via cytosolic and/or endosomal receptors [30–32]. TLRs in hosts serve as key receptors in these interactions by recognizing microbial components and triggering immune responses. TLRs 3, 7, 8, and 9, which are primarily located in host endosomal compartments, can detect viral products [33]. For example, TLR3 recognizes the double-stranded RNA (dsRNA) found in viruses and replicative intermediates of single-stranded RNA and DNA viruses [34, 35]. Further, TLR3 activation enhances the host's defense against potential pathogens and serves as a signaling hub for modulating inflammation, cell proliferation, and tissue regeneration [36–38]. TLR3 has been recognized as an important mediator in skin wound healing by activating a cascade of immune and reparative processes [8]. *Staphylococcus aureus* tRNA, for instance, induces type I interferon production via TLR7 activation in peripheral blood mononuclear cells [39]. Further, *S. aureus* EVs containing RNA and DNA can resist degradation and be delivered to host cells, where they modulate immune responses [32]. This suggests that RNA cargo in bacterial EVs may influence wound healing by regulating host immune responses. Moreover, commensal bacteria have shown promise in accelerating wound closure in preclinical studies, offering potential therapeutic applications in wound care [40]. In the present study, we aimed to investigate the role of Sm EVs in skin wound healing and identify specific EV cargo that contributes to this effect.

Materials and methods

Reagents

Anti-EGFR (clone D38B1, 4267), anti-phospho-EGFR (clone 53A5, 4407), anti-phospho-FAK (clone D20B1, 8556), anti-EEA1 (clone C45B10, 3288), anti-paxillin (clone E6R6Z, 50195), anti-Src (clone 36D10, 2109), anti p-Src (clone D49G4, 34069), and anti-rabbit IgG-HRP (7074) were provided from CST (Cell Signaling Technology, MA, USA). Anti-cytokeratin 13 (KRT13, 10164-2-AP), and anti-β-actin (20536-1-AP), anti-CD3 (17617-1AP), and anti-CD45 (20103-1-AP) were provided from Proteintech (IL, USA). Anti-phospho-TLR3 (NBP2-24904) was supplied from Novus, and anti-TLR3 (GTX113022) was acquired from GeneTex (CA, USA). Anti-FAK (sc-558), anti-mouse IgG-HRP (sc-2005), and anti-goat IgG-HRP (sc-2020) were provided by Santa Cruz Biotechnology (Santa Cruz, CA, USA).

Bacterial culture, EV isolation, and characterization

Streptococcus mutans (KCTC 3065, ATCC 25175) and *Escherichia coli* (K12 strain) were purchased from the

Korean Collection for Type Cultures (KCTC) institution. Bacteria were cultured until the optical density, measured at 600 nm, reached 1.5 OD in a brain heart infusion medium containing 3 μg/mL of vitamin K and 5 μg/mL hemin under an aerobic environment at 37°C. The isolation of EVs from *S. mutans* was performed as previously described [26, 41]. Briefly, bacterial cultures were centrifuged at 6000 g for 20 min, and the subsequent pellets were discarded. The supernatants were filtered using a 0.22 μm pore filter (Merck Millipore, Germany). The supernatants were concentrated using a tangential flow filtration (TFF) system (Biomax®100 kDa, Millipore, MA. USA). The filtrate was pelleted by ultracentrifugation in a 45 Ti rotor (Beckman Coulter, CA. USA) at 100,000 g and 4°C for 2 h. The final pellets were resuspended in phosphate-buffered saline (PBS) and stored at -80°C. Ec EVs were isolated using ExoBacteria EV Isolation kits (SBI, CA. USA) according to the manufacturer's protocol, as described previously [42]. The quality of the EVs was assessed by TEM (HT7700, Hitachi, Japan), as described previously [43]. Particle size and concentration of isolated bacterial EVs were analyzed using a Nanosight NS 300 System (Malvern Panalytical, Singapore).

Human oral organoid culture and proliferation analysis

Human oral tissues (buccal mucosa, tongue, and mandible mucosa) were provided from Kyungpook National University Hospital. Tissue processing and organoid culturing were performed as described by previous reports [44–46]. Primary tissue pieces were washed with 45 mL of ice-cold Advanced DMEM/F12 medium supplemented with 1× GlutaMAX, penicillin–streptomycin, 10 mM, and 100 μg/mL Primocin. Tissue pieces were crushed into small 1–3 mm^3 fragments in a 10 cm cell culture dish using surgical scissors or scalpels. Minced tissue samples were digested for < 1 h via incubation in TrypLE. When the mixture became cloudy, it was centrifuged at 200 × g and 4°C for 5 min, and the pellets were resuspended in 10 mL of medium and filtered using a 100 μm cell strainer. The samples were centrifuged again at the same conditions and the pellets were resuspended in cold Basement Membrane Extract (BME). Each 10 μL droplet was plated on culture plates. After seeding, the plates were incubated at 37°C for 30 min to allow the BME to solidify. Prewarmed organoid medium containing 1× B27 supplement was subsequently added to each plate. The medium was changed every 2–3 days, and organoids were split once every 1–2 weeks. Organoids were monitored using a Nikon ECLIPSE Ti microscope (Nikon Imaging Japan Inc.).

For cell proliferation and migration analysis in organoids, bacterial EVs were treated for 7 days. To evaluate the effect of specific antagonists for EGFR or TLRs, organoids were treated antagonists for 4 h, followed by treatment with Sm EVs for 7 days. Morphological changes were observed using phase-contrast microscopy.

Wound healing assay

Primary cultured human oral epithelial cells were incubated in a 24-well culture dish for the scratch assay. After the cells were attached, a 200 μL sterile pipette tip was used to create a wound line across the bottom of the dish. After washing with PBS, cells were treated with 10^7 particles/mL of bacterial EVs for 5 days. Then, wound closure size was defined using a bright field microscope.

Cell migration ability was tested in 24-well plates containing Transwell chambers (8 μm pore size) (Corning, CA. USA). Cells were suspended in a serum-free medium and added to the upper chamber. Medium containing 10^7 particles/mL of bacterial EVs was loaded into the lower chamber. Following incubation for 24 h, non-migrated cells on the upper surface of the inserts were removed gently using a cotton swab. The migrated cells were fixed using 4% paraformaldehyde and stained with 0.1% crystal violet solution. Cells were counted in five random separate optical fields.

RT-qPCR and western blot analyses

Total RNA was isolated using the phenol–chloroform extraction method with TRIzol reagent. The complementary DNA (cDNA) was synthesized from RNA using the 5 x CellScript cDNA Master kit (CellSafe, D-100, South Korea) following the manufacturer's protocol. Subsequently, the expression level of TLR3 was measured. The threshold cycle (Ct) values of quantitative PCR were determined using an ABI 7500 PCR system (Applied Biosystems, MA. USA) with TOPreal SYBR Green qPCR PreMIX (Enzynomics, RT500S, South Korea). GAPDH was used as the internal control. Primer sequences used in the analyses are as follows: TLR3, forward: TGTCTC ACCTCCACATCCTT, reverse: AACTGGGATCTCGT CAAAGC; GAPDH, forward: AGATCATCAGCAATGC CTCCTG, reverse: CTGGGCAGGGCTTATTCCTTTT CT. Matrigel-embedded organoids were treated with cell recovery solution at 4°C for 1 h, then collected by centrifugation. The protein concentration was measured after recovering the total protein using the protein extraction solution, and Western blotting was performed. β-actin was used as an internal control.

Transfection of SiRNA

Human oral mucosal organoids were transfected with a siRNA mixture comprising 2–3 specific oligonucleotides (Santa Cruz Biotechnology, CA. USA). Organoids were transfected using Lipofectamine 3000 (Thermo Fisher Scientific, L3000015) alongside the tested or control siRNA at a final 10 nM concentration. All transfection

steps were followed according to the manufacturer's protocol.

Electroporation of tRNA oligomers into EVs

For the delivery of specific oligomers into *E. coli* EV (Ec EV), synthesized oligomers were electroporated into EVs under conditions of V = 150 and C = 100 μF [42]. Following electroporation, the EVs were transferred onto ice. Then, RNase A was treated at 37°C for 30 min.

In vivo mouse assay

Four-week-old BALB/c black mice (male, weighing 20 ± 2) were stabilized for 2 weeks. After the mice were shaved for the wounding experiments, four full-thickness open wounds were performed on the dorsal skin of anesthetized 8 mice using a sterile 4 mm-diameter punch device [47, 48]. The mice were randomly divided into two groups, and each wound was treated daily with 10 μL of EV solution (10^7 particles/mL) in the experimental group or with 10 μL of PBS in the control group until day 4 or 6. The treatment solution was allowed to dry before the mice were returned to their cages. The wound area was compared after EV treatment for 6 days. Each control or experimental group consisted of 16 wounds. Additionally, the experiment consisted of treating scars with specific RNA oligomers electroporated in Ec EV*s*. To minimize variability, wound area measurements were performed under blinded conditions. At each designated time point, mice were temporarily anesthetized and positioned at a fixed distance from a calibrated digital camera mounted on a stand. Images were captured without applying pressure or tension to the wound site to avoid artificial contraction. The wound area was then quantified using metric ruler in the images. TLR3 KO mice (weighing 20 ± 2, The Jackson Laboratory, Nar Harbor, ME. USA) were also used in this trial. There were 10 wounds in each group. EVs were treated for 4 days, and histopathological methods were employed to analyze skin samples.

IF and IHC staining

To make a frozen organoid section, the organoid was embedded by Surgipath FSC 22 Frozen section compound (Leica Biosystems, Nussloch, Germany) at -80 °C. The organoid was sectioned to a thickness of 20 μm on the slide, following permeabilization using 0.1% Triton X-100 for 15 min and blocked in 1% (bovine serum albumin) BSA containing 0.01% Triton X-100. Each sample was incubated with primary antibodies at 4 °C overnight. DAPI was also stained to identify the nucleus. All samples were determined using a LSM 700 confocal microscopy system (ZEISS, Oberkochen, Germany). To confirm that the Sm EV RNA cargo is delivered to the endosomes within cells where TLR3 is mainly distributed, EV RNA was stained using the RNA-specific SYTO RNASelect dye (Thermo Fisher Scientific, MA. USA), and incubated with organoids for 10 min. Organoids were subsequently fixed and IF-labeled for the early endosomal marker EEA1.

For a more precise evaluation of the wound healing process, we performed histological analyses of the wound area at the endpoint of the experiment. The obtained sections were fixed using 4% paraformaldehyde at room temperature for 5 min. The fixed samples were then washed with PBS and permeabilized using 1% Tween-20 in PBS for 5 min. The samples were incubated with 1% BSA in PBS for 2 h and subsequently with specific antibodies (1:500) at 4 °C overnight. The IHC staining was performed using the UltraTek HRP Anti-Polyvalent kit (AMF080, ScyTek Laboratories, UT. USA). Tissues were counterstained using hematoxylin and eosin. Images were captured using a ZEISS Axio microscope (ZEISS Microscopy, Germany).

EV RNA sequencing and oligomer synthesis

The collected EVs were treated with RNase inhibitor (Applied Biosystems) at 37 °C for 15 min. Next, RNAs from EVs were isolated using the miRNeasy kit (Qiagen, Germany) according to the manufacturer's protocols. RNA quality was confirmed by a 2100 Bioanalyzer (Agilent Technologies, CA. USA), and the SMARTer smRNA-Seq kit (Takara Bio, Japan) for Illumina was used to sequence EVs RNA, following the manufacturer's protocol. The libraries were validated using the Agilent Bioanalyzer and sequenced on an Illumina NovaSeq instrument. The RNA oligomers were synthesized by Macrogen, Inc. (South Korea).

Statistical analysis

All *in vitro* experiments were performed independently at least twice. Statistical parameters, including analysis of the *in vivo* results obtained from the murine models, are presented in the figure legends. All statistical analyses were conducted using the Excel Analysis ToolPak. One-way ANOVA analysis and unpaired t-test were used for the statistical testing of comparisons between three or more and two groups, respectively. A p-value < 0.05 was considered statistically significant. Significant p-values are shown in each figure.

Results

Isolation and characterization of Sm EVs

Transmission electron microscope (TEM) revealed that the isolated EVs exhibited a spherical morphology (Fig. S1A). Nanoparticle tracking analysis (NTA) provided further insights into the heterogeneous size distribution of the EVs ranging between 50 and 400 nm (Fig. S1A). SDS-PAGE analysis on both bacterial pellets and isolated EVs demonstrated that the EVs encapsulated distinct proteins

that differed from those in the *S. mutans* cells of origin (Fig. S1B).

Sm EVs promote epithelial cell proliferation and migration in mucosal organoids

We cultured organoids from human oral mucosal tissues, including the tongue, buccal, and mandibular regions. Immunofluorescence (IF) staining with anti-KRT13, a marker of oral epithelial cells, confirmed the identity of the organoids (Fig. S2A). To assess the uptake of Sm EVs by the organoids, we incubated the organoids with pre-labeled EVs using fluorescent dyes. After 24 h of incubation, EV membranes (DiD) and intra-EV RNA (sytoRNA) were detected within the organoids (Fig. S2B).

We observed that Sm EVs induce the migration of epithelial cells in buccal mucosal organoids. This phenomenon closely resembles the migration and attachment to the base of the culture dish, as reported by Chakrabarti et al. in gastric organoids [49]. As shown in Fig. S2C, all groups show relatively similar morphology at Day 0. By Day 7, in the control group (0 particles/mL), the organoids maintain a compact structure with minimal morphological alterations. However, at higher concentrations (10^6–10^8 particles/mL), the organoids appear more dispersed and pronounced spreading (marked by arrows), suggesting Sm EV-dependent migration of organoids' cells. Based on these results, we selected a concentration of 10^7 particles/mL for subsequent experiments.

We treated organoids from three different mucosal tissue types with 10^7 particles/mL of Sm EVs for 7 days. Phase-contrast microscopy revealed increased cell migration in the treated organoids compared to the controls (Fig. 1A). To confirm that the cell migration from the organoids was due to increased cell proliferation, we performed IF staining using an anti-Ki67 antibody, a cell proliferation marker. Organoids treated with Sm EVs for 24 h exhibited significantly higher Ki67 expression than the control group (Fig. 1B).

Sm EVs promote wound healing in mouse dorsal skin

Because the wound healing process relies on epithelial proliferation and migration [50, 51], we conducted *in vivo* experiments to evaluate Sm EVs' wound healing potential. On day 1, the Sm EV-treated mouse group exhibited a significantly reduced wound area compared to the PBS control group, with this trend persisting to day 6 (Fig. 2A). Following the sacrifice of the mice, histological analysis of the wound tissues was performed to evaluate the epithelial remodeling using H&E staining. In the PBS group, incomplete re-epithelialization was observed, with a thinner and irregularly regenerated epidermis. Below the epidermis, dermal detachment and granulation tissue were observed, indicating that the wound healing process was still ongoing. In contrast, the Sm EV-treated group demonstrated a marked improvement in wound healing, with a relatively uniform epidermis and a dense dermis, rather than the presence of granulation tissue in the dermal layer (Fig. 2B).

TLR3 is involved in Sm EV-dependent acceleration of cell proliferation

It is well-established that TLRs are involved in the interaction between bacterial EVs and host cells. To identify which TLR is responsible for Sm EV-mediated cell proliferation and migration, we used specific agonists for TLR2, TLR3, and TLR7/8 (Pam3CSK4, poly I: C, and R-848, respectively), which mainly recognize Gram-positive bacterial components. Agonists for TLR2 and TLR7/8 showed no significant effect on cell migration over 7 days (Fig. 3A). However, the TLR3 agonist poly I: C significantly enhanced cell proliferation and migration, mirroring the effects of Sm EVs (Fig. 3B). Moreover, pretreatment with the TLR3 antagonist CU-CPT-4a abolished both Sm EV- and poly I: C-mediated cell proliferation and migration (Fig. 3B). Sm EV treatment led to a marked increase in TLR3 phosphorylation (Fig. 3C, left two lanes). In contrast, TLR3 phosphorylation was suppressed when the cells were pretreated with the TLR3 antagonist (Fig. 3C, right two lanes). TLR3 knockdown via siRNA yielded similar results, confirming that TLR3 is essential for Sm EV-mediated cell proliferation and migration (Fig. 3D). We used IF staining to confirm that the Sm EV RNA cargo was delivered to the cellular endosomes, where TLR3 is predominantly localized. EV RNA (sytoRNA) and early endosomes (EEA1) in organoids were labeled with specific markers. Confocal microscopy revealed substantial colocalization between EV RNA and the endosomal marker, suggesting successful delivery of Sm EV RNA to the endosomes (Fig. 3E).

EGFR is involved in Sm EV-mediated acceleration of cell proliferation

The epidermal growth factor (EGF) signaling pathway is crucial for epithelial cell proliferation [52, 53]. Moreover, TLR3 signaling from the endosomal membrane is closely associated with EGFR [54]. Therefore, we investigated whether the EGFR activation contributes to the Sm EV-mediated increase in cell proliferation. Sm EVs enhanced EGFR phosphorylation (Fig. 4A), and pretreatment with EGFR inhibitors such as gefitinib and afatinib significantly reduced Sm EV-mediated EGFR phosphorylation (Fig. 4B) and cell proliferation/migration (Fig. 4C) in the organoids. Additionally, pretreatment with siTLR3 diminished Sm EV-induced EGFR phosphorylation, indicating that TLR3 plays a crucial role in Sm EV-mediated EGFR activation (Fig. 4D).

Given that EGFR activation is a critical signaling pathway in the progression of oral squamous cell carcinoma

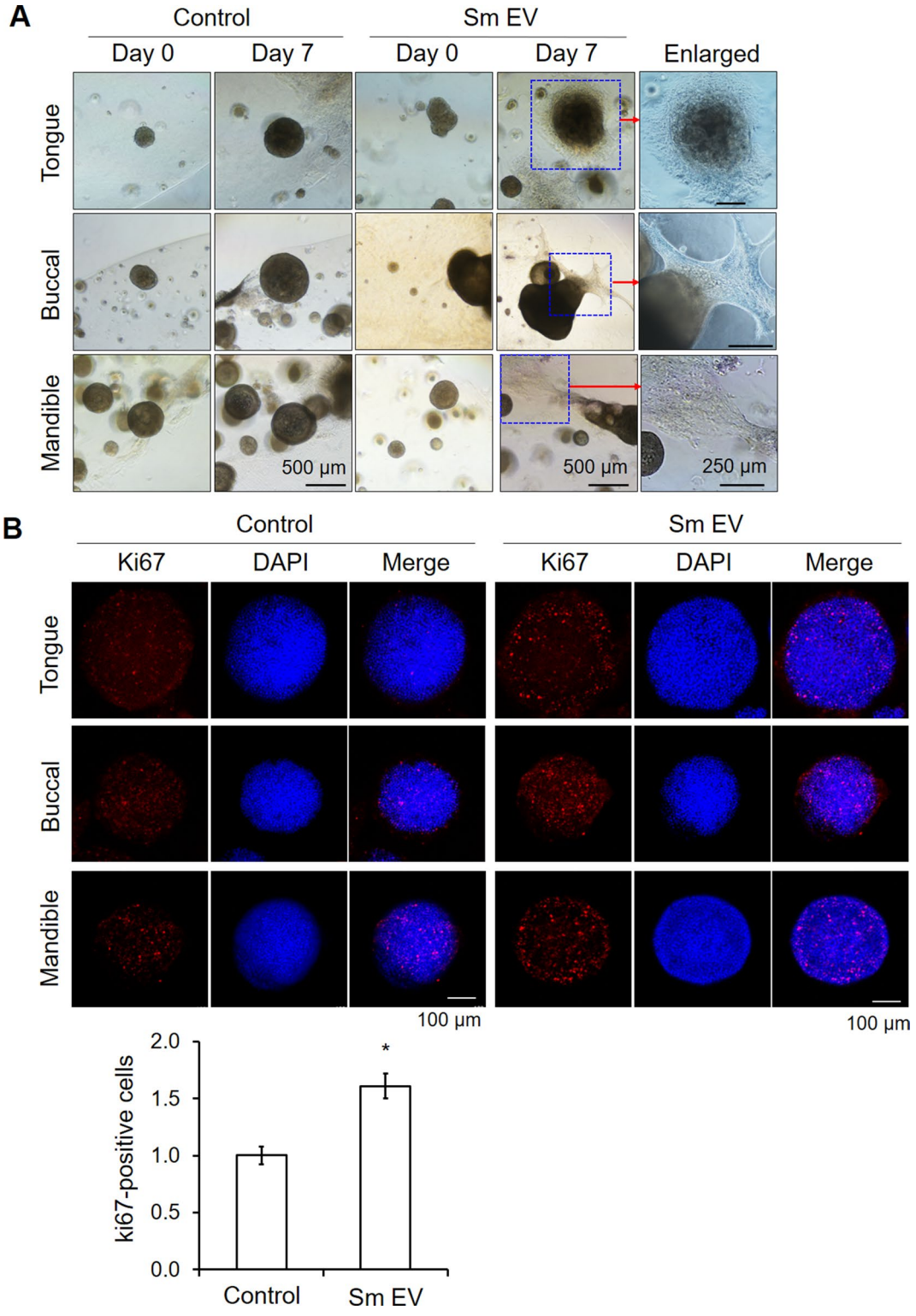

Fig. 1 Effect of Sm EVs on cell proliferation and migration in mucosal organoids. (**A**) Organoids derived from three oral mucosal tissues were treated with 10^7 particles/mL of Sm EVs for 7 days. Organoid morphology was monitored using phase-contrast microscopy. (**B**) Confocal microscopy images showing Ki67 (red) expression, a cell proliferation marker, in organoids treated with Sm EVs for 24 h. DAPI (blue) staining was used as a nuclear control (*$p < 0.05$).

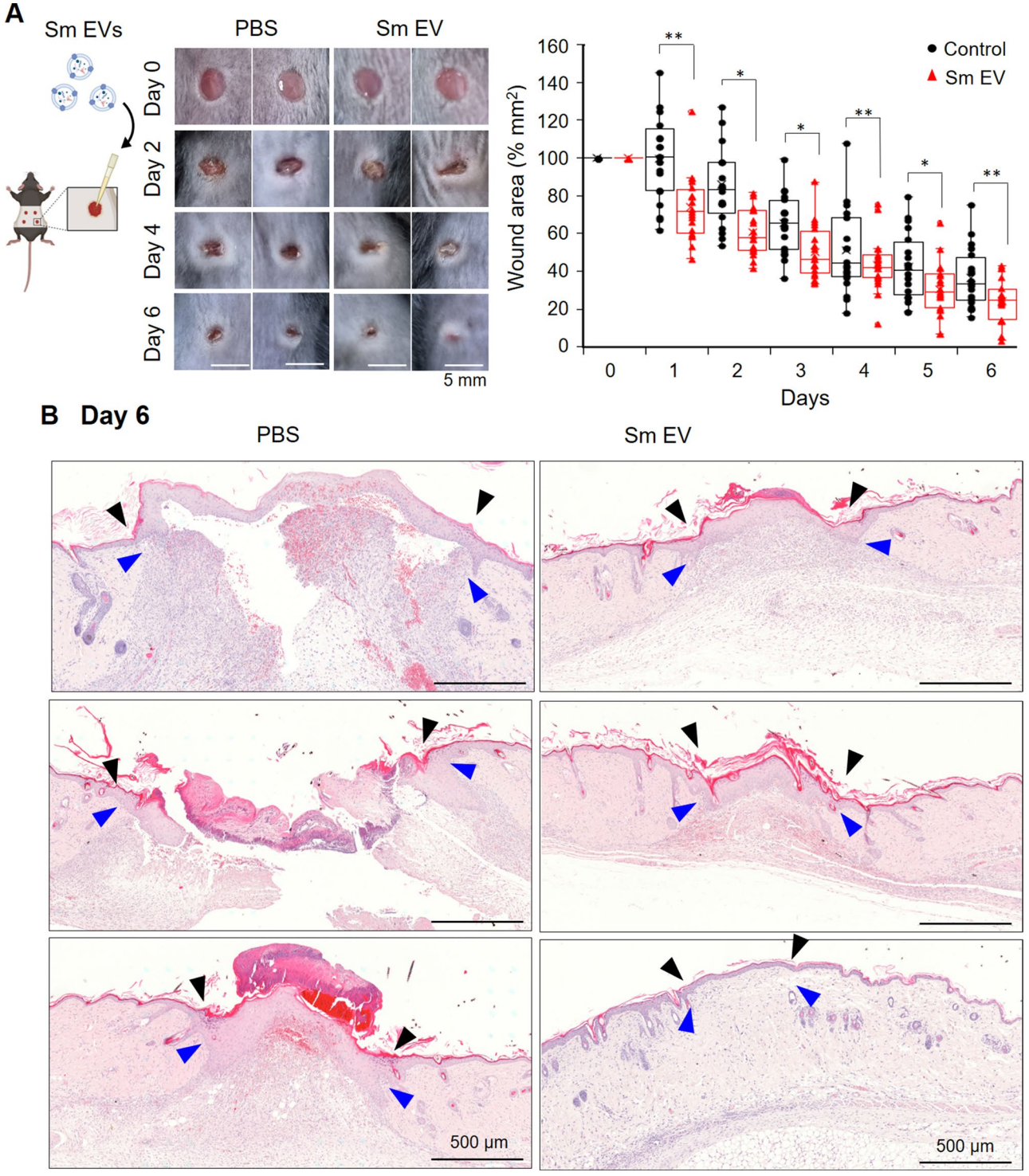

Fig. 2 Effect of Sm EVs on wound healing in mouse dorsal skin. (**A**) A 4 mm punch device was performed to create wounds on the dorsal surface of the mice, which were then randomly assigned to two groups. The experimental group received 10 μL of Sm EV solution (10^7 particles/mL in PBS) daily for 6 days, while the control group received 10 μL of PBS. Diagrams were created with BioRender.com. Wound areas were photographed and measured daily using a metric ruler in the images (*$p < 0.05$, **$p < 0.01$). Data are presented as the mean ± standard deviation. (**B**) After 6 days of treatment, the mice were sacrificed, and wound tissues were subjected to histological analysis using H&E staining. Arrows indicate the wound area.

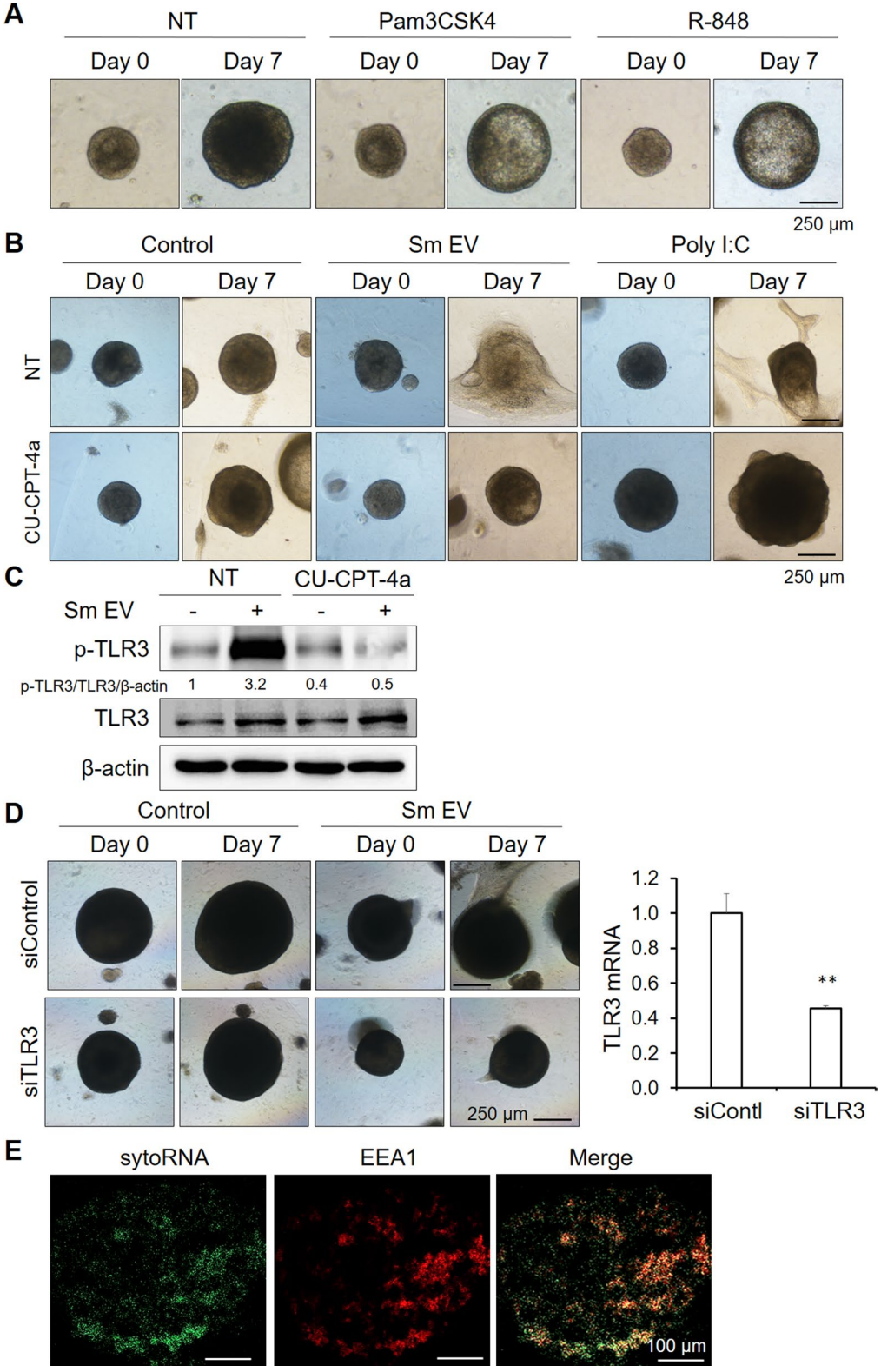

Fig. 3 (See legend on next page.)

(See figure on previous page.)

Fig. 3 TLR3-dependent cell proliferation induced by Sm EVs. (**A**) Organoids were pretreated with specific TLR agonists for 4 h and treated with Sm EVs (10^7 particles/mL) for 7 days. Morphological changes were monitored using phase-contrast microscopy. (**B**) Organoids were pretreated with the TLR3 antagonist (CU-CPT-4a) for 4 h, followed by treatment with Sm EVs or the TLR3 agonist (poly I: C) for 7 days. Morphological changes were observed using phase-contrast microscopy. (**C**) TLR3 phosphorylation (Tyr 759) was evaluated by Western blot analysis under the same conditions. (**D**) Organoids were transfected with 10 μM of control siRNA or siTLR3 for 24 h, followed by treatment with Sm EVs for 7 days. TLR3 knockdown efficiency on day 7 was confirmed by qPCR (**$p < 0.01$). (**E**) EV RNA was stained using the RNA-specific SYTO RNASelect dye (green) and incubated with organoids for 10 min. The organoids were fixed and treated with antibody against an early endosomal marker EEA1 (red), then analyzed by confocal microscopy.

(OSCC), a common oral cavity malignancy [55], we evaluated cell proliferation in OSCC organoids treated with Sm EVs for 7 days. Organoids derived from UMSCC1 cell line's xenografts or tongue cancer tissues did not show significant epithelial cell proliferation or migration upon Sm EV treatment (Fig. S3A). Furthermore, human tongue cancer tissues exhibited no notable phosphorylation of EGFR in response to Sm EV treatment (Fig. S3B). These findings suggest that Sm EVs promote epithelial cell proliferation only in non-tumorigenic mucosal organoids.

Sm EVs enhance focal adhesion and wound healing via TLR3

We examined whether Sm EVs facilitate focal adhesion complex formation, a critical step in cell migration [56]. F-actin and paxillin, key cytoskeletal and scaffolding proteins, are recruited early to nascent focal adhesions at the leading edge of migrating cells and are essential for focal adhesion turnover during migration [57, 58]. We analyzed the dynamics of focal adhesion kinase (FAK) and actin filaments in organoids treated with Sm EVs for 24 h. Sm EV treatment led to FAK activation and subsequent focal adhesion complex formation, as shown by increased colocalization of paxillin (red) and actin (green), indicating focal adhesion-dependent migration at the cell leading edge (Fig. 5A, B). The white-boxed regions in Fig. 5A provide an enlarged view of these interactions. Furthermore, TLR3 knockdown reduced Sm EV-induced FAK phosphorylation, demonstrating that TLR3 plays a key role in enhancing cell proliferation and migration in response to Sm EV-dependent FAK activation (Fig. 5C). In human tongue cancer tissues, there was no notable phosphorylation of FAK in response to Sm EV treatment (Fig. S3C).

Sm EV total RNA sequencing

RNA is likely one of the key cargos in Sm EVs, which allows them to function as a ligand for the host cell's endosomal TLR3. Therefore, we performed total RNA sequencing on Sm EVs. The analysis revealed that RNAs with read counts exceeding 100 were identified as small RNA sequences ranging from 20 to 130 bp (Fig. S4). Notably, the five most abundant RNA species identified in Sm EVs were all tRNAs, as detailed in Table 1. To compare the structural characteristics of these tRNAs, we predicted their 3D structures using the trRosetta server, a deep-learning-based protein and RNA structure prediction tool that generates structural models based on predicted inter-residue distances and orientations. The predicted 3D structures of the tRNAs have been incorporated into Table 1, providing additional insights into their potential role as TLR3 ligands. The total RNA sequencing data for Sm EVs have been deposited in Bioproject: PRJNA1168705.

Sm EV-derived tRNA variants are crucial for promoting cell proliferation and migration

To explore whether the synthesized tRNA Oligos derived from Sm EVs contribute to promoting wound healing, we tested its effects on the proliferation and migration of primary oral epithelial cells. Because of the differences in cellular entry mechanisms, intracellular trafficking, and functional stability between bacterial EVs and synthetic carriers such as liposomes [59–61], we used bacterial EVs as a carrier for Sm EV-derived tRNA oligos. Our previous study demonstrated that *E.coli* EVs (Ec EVs) can serve as vehicles for delivering genetic material [42]. Therefore, we used Ec EVs with some preliminary experiments. First, Ec EVs did not significantly affect cell proliferation (Fig. S5A) and migration (Fig. S5B) even at a concentration of 10^7 particles/mL. In addition, the optimal copy number of synthesized tRNA-Met variants (Oligo 1 and Oligo 3) to be electroporated into Ec EVs was determined as follows. We loaded the oligos at various concentrations into Ec EVs (10^7 particles/mL) using electroporation, then treated primary oral epithelial cells with Ec EVs containing the oligos for 48 h and measured cell viability. Generally, the highest cell viability was observed when 10^{12} copies/mL (3 nM/mL) of oligos were transfected into the Ec EVs (Fig. S6A). Transwell migration assay showed that, when Oligo1 and 3 were loaded respectively into Ec EVs at 10^{12} copies/mL, cell migration levels markedly increased (Fig. S6B). In contrast, Oligos 2, 4, and 5 did not show notable effects under similar conditions.

Additional experiments were performed under the condition that 10^{12} copies/mL of Oligos was electroporated into 10^7 particles/mL of Ec EVs (Fig. 6A). We compared the effects of Oligo 1 and 3 on cell migration with Sm EVs using scratch assay. Ec EV alone did not enhance cell migration compared to Sm EV group. However, when Oligo1 and 3 were loaded respectively into Ec EVs, cell migration levels significantly increased, comparable to those observed with Sm EV treatment (Fig. 6B). This result was further corroborated by the Transwell

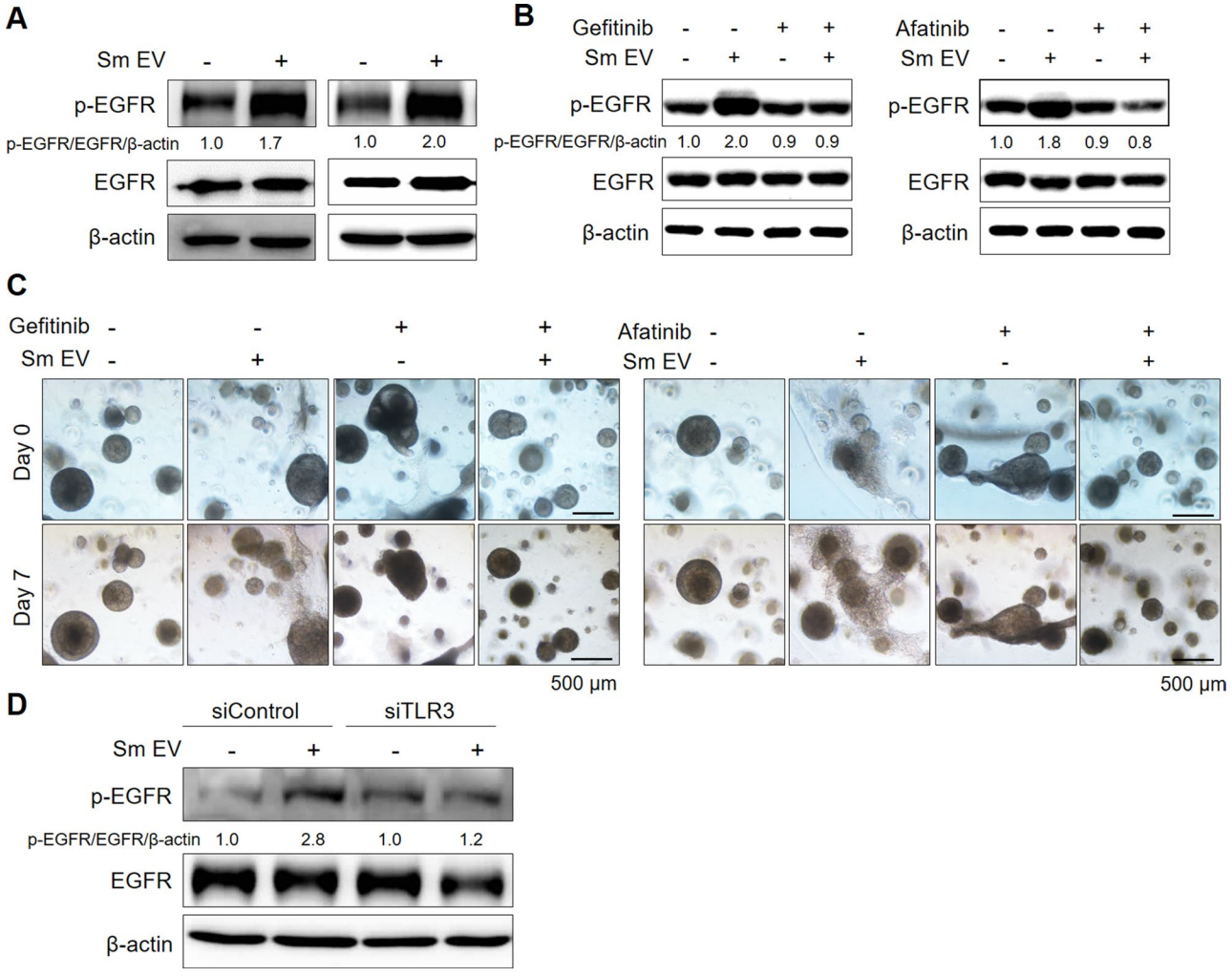

Fig. 4 Effect of Sm EVs on EGFR activation. (**A**) Two different types of organoids were treated with 10^7 particles/mL of Sm EVs for 3 days. EGFR phosphorylation was assessed using Western blot analysis. (**B**) Organoids were pretreated with EGFR inhibitors, gefitinib (1.1 μM) or afatinib (500 nM), followed by Sm EV treatment for 3 days. EGFR phosphorylation (Tyr 1173) was assessed using Western blot analysis. (**C**) Morphological changes in organoids treated under the same conditions were monitored for 7 days using phase-contrast microscopy. (**D**) Organoids were pretreated with control siRNA or siTLR3 for 24 h, followed by treatment with Sm EVs for 7 days. EGFR phosphorylation (Tyr 1173) was assessed using Western blot analysis.

migration assay, where Ec EVs loaded with Oligos 1 or 3 significantly promoted cell migration similar to Sm EVs (Fig. 6C). Additionally, in human primary oral mucosal organoids, treatment with Ec EVs carrying Oligos 1 or 3 promoted both cell proliferation and migration, whereas Ec EVs alone failed to induce these effects (Fig. S7).

To further investigate whether the wound healing effects of Sm EVs are specifically mediated by RNA cargo rather than other EV components such as membrane lipids, we conducted two additional control experiments. First, we delivered synthetic Oligo 1 using Lipofectamine. As shown in Fig. S8, Lipofectamine alone did not affect cell viability or migration compared to the PBS or Ec Ev control. However, when Oligo 1 was loaded into Lipofectamine, epithelial cell proliferation and migration significantly increased, comparable to the effects seen with Sm EVs or Ec Evs carrying Oligo 1. This suggests that the observed wound-healing effects are primarily attributable to the Oligo 1, rather than other components of Sm EVs. Second, we examined the effect of heat-inactivated Sm EVs, in which RNA and protein components were denatured by thermal treatment. Heat-treated EVs failed to promote epithelial cell proliferation or migration, both in native Sm EVs (Fig. S9A) and in Ec EVs carrying Oligo 1 (Fig. S9B). These findings suggest that intact RNA cargo is essential for the biological activity of Sm EVs. Collectively, these results support the hypothesis that tRNA cargo, rather than lipids or other non-specific components of Sm EVs, plays a key role in mediating their wound healing effects.

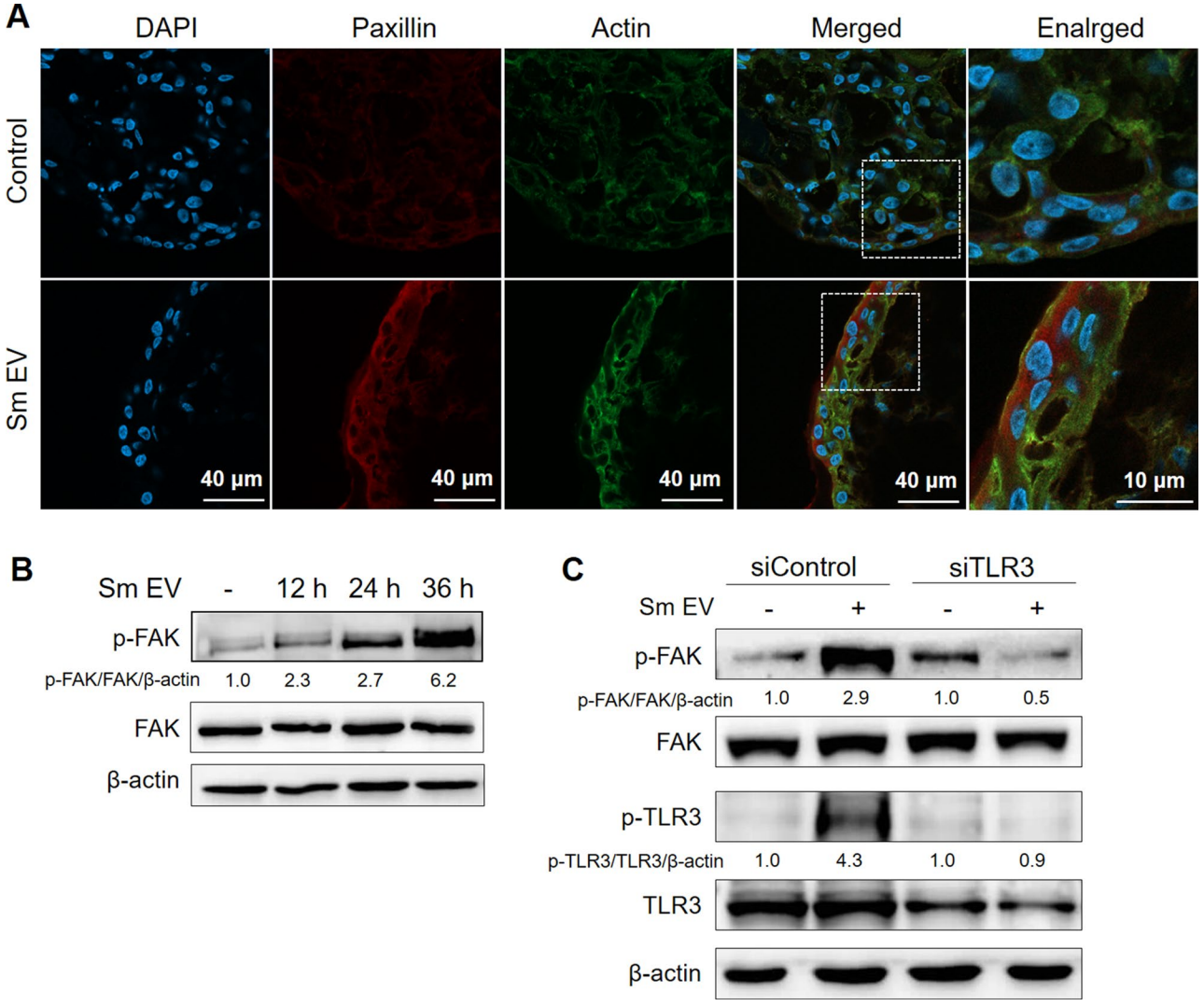

Fig. 5 Effect of Sm EVs on focal adhesion activation. (**A**) Organoids were treated with 10^7 particles/mL of Sm EVs for 24 h. Paxillin (red) and F-actin (green) were stained and visualized using confocal microscopy. The boxed regions represent enlarged views on the right. (**B**) FAK phosphorylation (Tyr 397) was evaluated by Western blotting in organoids treated with Sm EVs for 36 h. (**C**) Organoids were transfected with siTLR3 for 24 h, followed by treatment with Sm EVs for an additional 24 h. Protein expression and phosphorylation levels were determined by Western blot analysis.

Sm EV-derived tRNA variant promotes focal adhesion complex formation

We analyzed the focal adhesion complex formation in organoids treated with Ec EVs or Oligo 1-transfected Ec EVs for 24 h. Ec EVs carrying Oligo 1 led to focal adhesion complex formation, as shown by increased colocalization of paxillin (red) and actin (green) (Fig. 7A). The white-boxed regions in Fig. 7A provide an enlarged view of these interactions. Next, we investigated the activation of Src kinase and FAK with treatment of Sm EVs and Ec EVs carrying Oligo 1. As shown in Fig. 7B, there was a significant increase of phosphorylation of Src and FAK upon treatment with Sm EVs and Ec EVs carrying Oligo 1. This suggests that Src activation is involved in the signaling cascade leading to FAK activation.

Sm EV-derived tRNA variant enhanced skin wound healing in mice model

To investigate the wound healing effect of Sm EV-derived tRNA variant in a mouse model, synthesized Oligo 1 was electroporated into Ec EVs and applied to dorsal skin wounds (Fig. 8A). Control groups were treated with PBS and Ec EVs without Oligo 1. After 4 days of treatment, the wound areas in both the PBS- and Ec EV-treated groups were comparable, showing no significant difference. In contrast, the group treated with Ec EVs carrying Oligo 1 exhibited a significantly reduced wound area compared to both control groups (Fig. 8B). Following the sacrifice of the mice, H&E staining was performed to monitor epithelial remodeling. As shown in Fig. 8C, the Ec Ev-Oligo 1 group, similar to Sm EV group, exhibited a relatively uniform epidermis and a dense dermis,

Table 1 Summary of oligomers synthesized with the five most abundant tRNA sequences among Sm EV small RNAs

Small RNA	Oligo no.	bp	Read count	Sequence	3D structure*
tRNA-Met	Oligo 1	76	20276	CGCGGGAUGGAGCAGUUA GGUAGCUCGUCGGGCUCA UAACCCGAAGGUCGUAGG UUCAAAUCCUGCUCCCGCA ACC	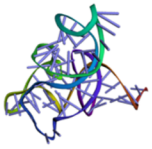
tRNA-Ile	Oligo 2	76	13701	GGGCGCGUAGCUCAGCUG GUUAGAGCGCACGCCUGA UAAGCGUGAGGUCGGUGG UUCGAGUCCACUCGUGCC CACC	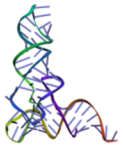
tRNA-Met	Oligo 3	75	7960	GCGGGAUGGAGCAGUUAG GUAGCUCGUCGGGCUCAU AACCCGAAGGUCGUAGGU UCAAAUCCUGCUCCCGCAA CC	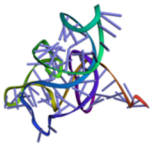
tRNA-Val	Oligo 4	75	7351	GGGAGUUUAGCUCAGUUG GGAGAGCAUCUGCCUUAC AAGCAGAGGGUCAGCGGU UCGAGCCCGUUAACUCCC ACC	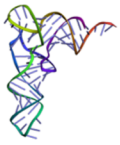
tRNA-Asn	Oligo 5	53	6319	AGCGCAUGACUGUUAAUCA UGAUGUCGUAGGUUCGAG UCCUACUGCCGGAGCC	

The 3D structures of tRNAs were predicted using the trRosetta based on predicted inter-residue distances and orientations. *Color by rainbow from purple (5'-terminus) to red (3'-terminus).

suggesting enhanced wound healing compared to the PBS and Ec EV control groups.

Sm EV-derived tRNA variant does not promote wound healing in TLR3 Knouckout mice

Next, a TLR3 knocukout (KO) mouse model was used to determine whether the wound healing effect of Sm EV-derived Oligo 1 were mediated through TLR3. In contrast to wild-type mice, applying Ec EVs loaded with Oligo 1 to TLR3 KO mice did not promote significant differences in wound healing rates compared to the PBS or Ec EV control groups (Fig. S10A). H&E staining of wound tissues collected after 4 days of treatment revealed no noticeable differences in healing progression across the three groups (Fig. S10B). These results suggest that TLR3 plays a crucial role in the wound healing mechanism promoted by Sm EV-derived Oligo 1.

Discussion

Oral wound healing is considered an ideal model because it occurs rapidly and without scar formation. Although the general tissue architecture of skin and oral mucosa shares similarities, there are notable histological differences [16]. Despite these differences, various efforts have been made to apply the rapid healing mechanism of oral mucosa to skin wounds [62, 63]. Therefore, by identifying the factors behind the enhanced wound healing capacity of the oral mucosa, we can explore methods to improve skin wound healing. Given the increasing demand for effective delivery systems and alternative approaches to promote healing and tissue remodeling, this study investigated the potential of EVs derived from oral bacteria as a novel strategy to accelerate skin regeneration. Among various candidates, commensal bacterial EVs have emerged as promising therapeutic agents due to their unique biological properties and ability to influence host processes [64]. Unlike the direct application of bacteria, which mainly affects localized colonization regions,

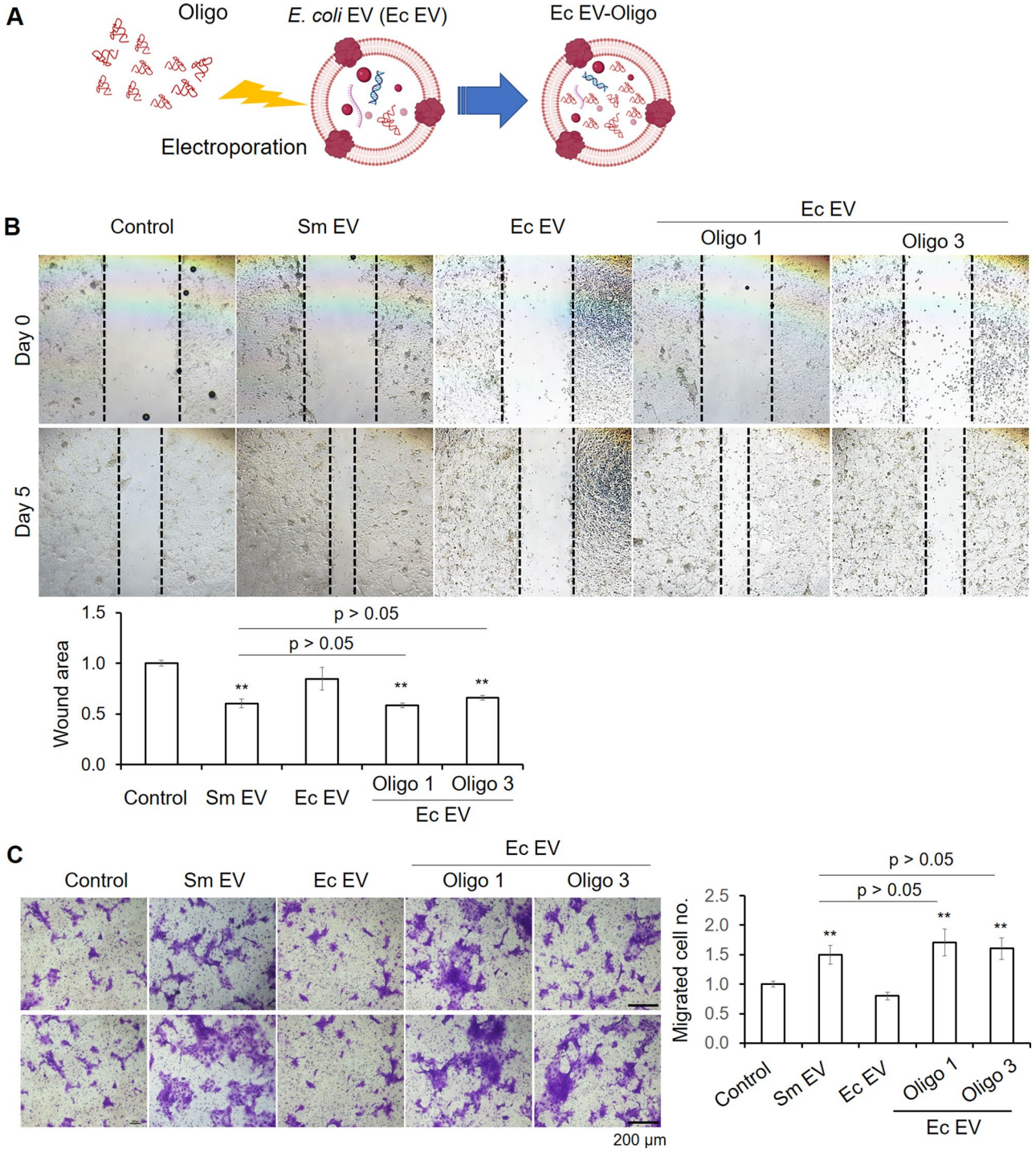

Fig. 6 Effect of Sm EV-derived tRNA oligos on primary oral epithelial cell migration. (**A**) A flow diagram illustrating the preparation of Ec EVs loaded with oligos synthesized from tRNA sequences derived from Sm EVs. Images were created with BioRender.com. (**B**) For the scratch wound-healing assay, confluent monolayers of primary oral epithelial cells in a 12-well plates were scratched with a pipette tip to create a wound. Cells were then cultured in the presence of Ec EVs with or without Oligos 1 or 3 for 5 days, and wound closure was measured over time. (**C**) For the Transwell migration assay, primary oral epithelial cells were treated with Ec EVs carrying specific oligos for 24 h. Migrated cells were stained using 0.2% crystal violet in 10% ethanol and counted under a phase-contrast microscope. $^{**}p < 0.01$

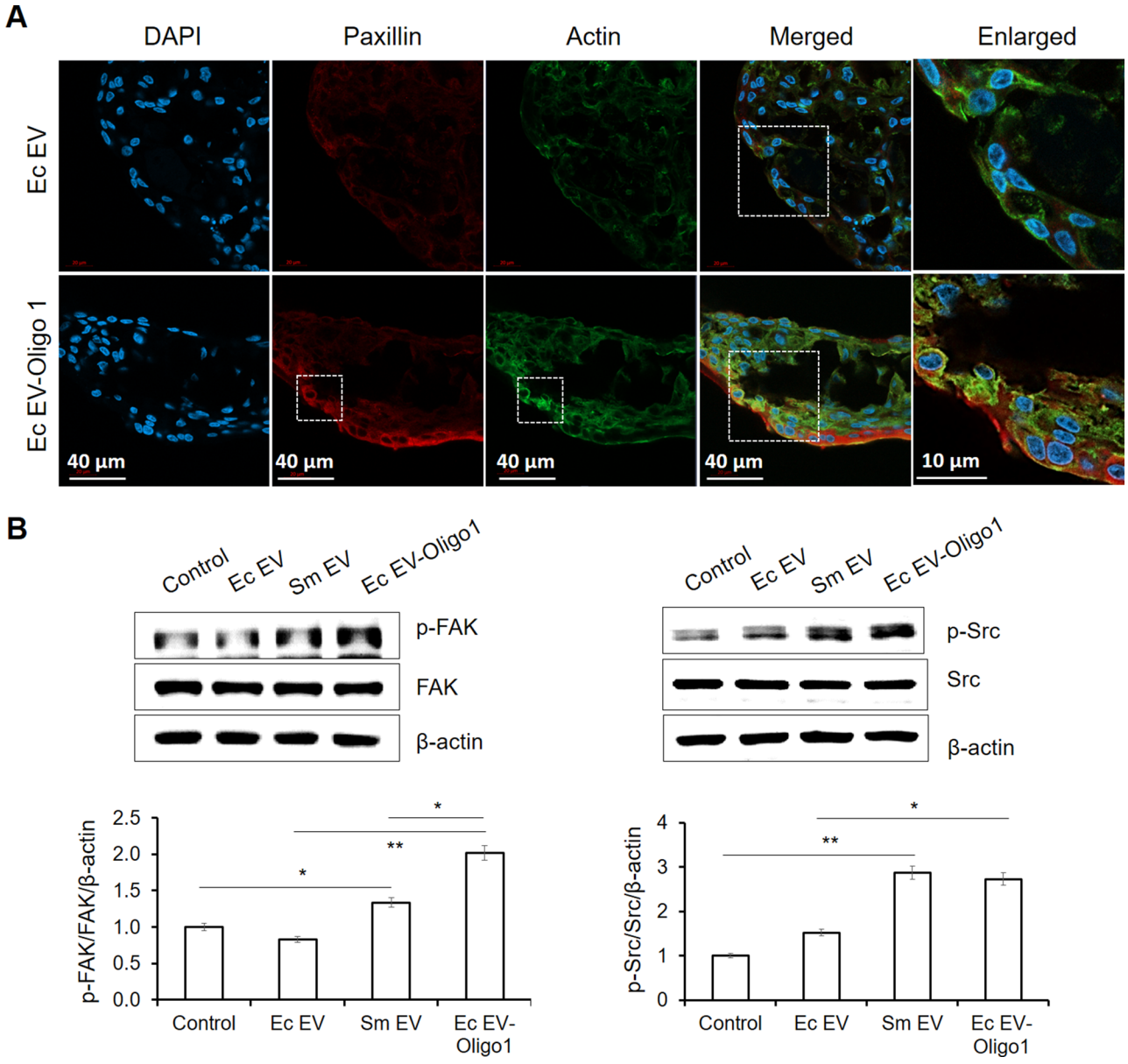

Fig. 7 Effect of Ec EVs carrying Oligo 1 on focal adhesion complex formation. (**A**) IF staining of paxillin (red) and F-actin (green) in organoids treated with Ec EVs or Ec EVs carrying Oligo 1 for 48 h. Confocal microscopy was used to visualize the colocalization of paxillin and F-actin. (**B**) Western blot analysis of Src phosphorylation (Tyr 416) and FAK phosphorylation (Tyr 397) in organoids treated with EVs for 48 h (*$p < 0.05$, **$p < 0.01$).

EVs are recognized for their critical role as signal carriers in normal and pathological processes. Moreover, the capacity of EVs for long-range signaling provides valuable opportunities to explore their functional biology and regulatory mechanisms in wound healing. Apart from EVs, microbes can deliver RNA through other mechanisms, such as releasing naked RNA during cell death or through active secretion [65, 66]. However, such RNAs are highly vulnerable to rapid degradation due to the abundant ribonuclease (RNase) activity present in the extracellular milieu [67]. Conversely, EVs can protect the RNA cargo, thus facilitating RNA transport over longer distances without degradation [68, 69]. This suggests that EVs may have an active RNA-sorting mechanism that selectively packages and protects specific RNAs. While much remains to be explored in this area, the potential for EVs to deliver functional RNAs highlights promising possibilities for therapeutic applications.

Recent advances in high-throughput sequencing have revealed the extensive involvement of non-coding RNA (ncRNA) in gene regulation across both prokaryotes and eukaryotes [70–72]. Indeed, growing interest in bacterial extracellular RNAs has emerged due to their potential roles in bacterial–host interactions. Among these,

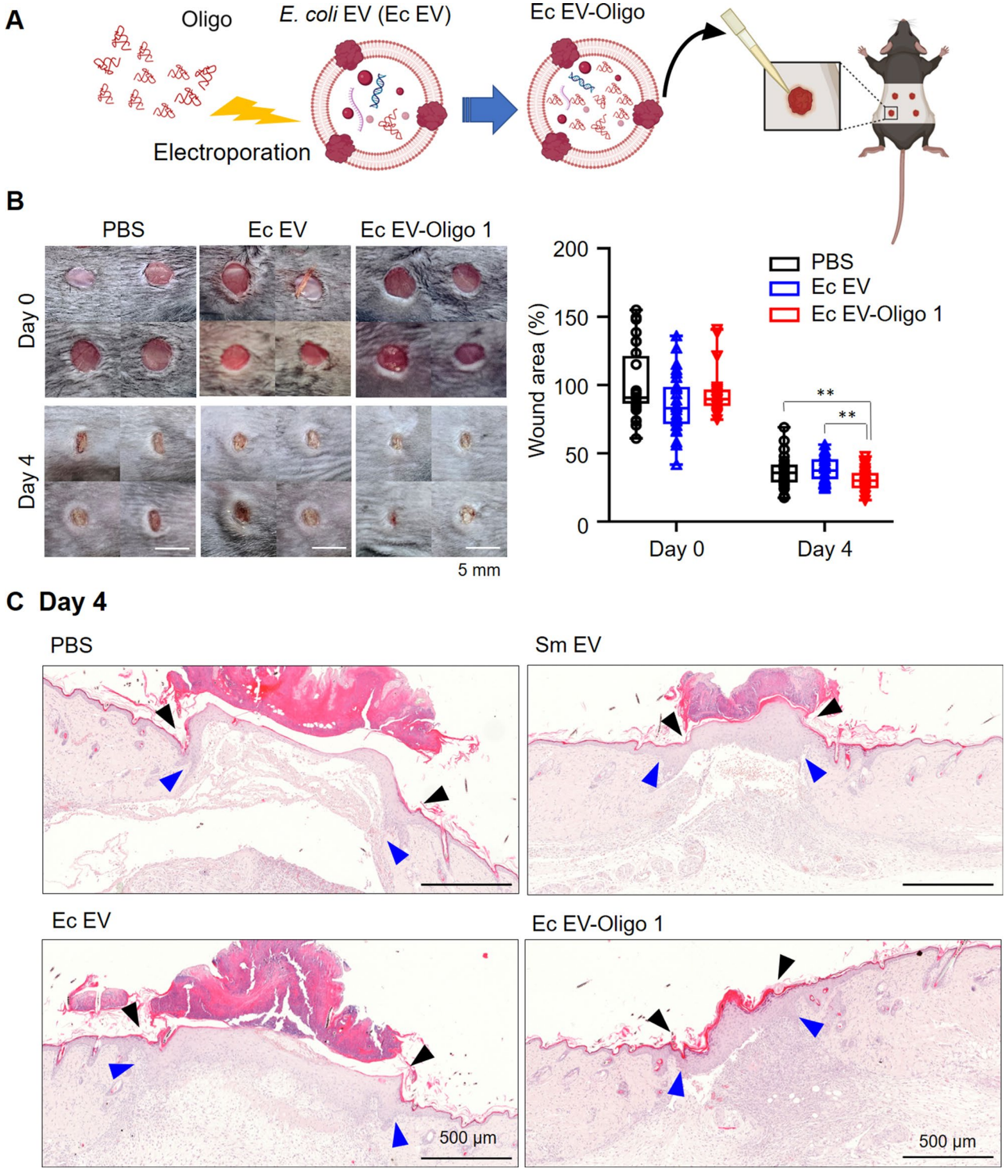

Fig. 8 Effect of Sm EVs-derived tRNA Oligo 1 on wound healing in mouse dorsal skin. (**A**) A flow diagram illustrating the mouse skin wound healing assay including preparation of Ec EVs loaded with Oligo 1. Images were created with BioRender.com. (**B**) Representative images of mouse wounds treated with PBS, Ec EVs, and Ec EVs carrying Oligo 1 taken on days 0 and 4. After the dorsal epidermis of each mouse was wounded using a 4 mm punch device, the mice were randomly divided into three groups. Each wound was treated daily with 10 μL of Ec EV with or without Oligo 1 (10^{12} copies/mL) in the experimental group or 10 μL of PBS in the control group until day 4 ($n = 16$ wounds per group). The wounds were photographed and measured using a metric ruler (**$p < 0.01$). (**B, C**) After 4 days of treatment, the mice were sacrificed, and wound tissues were subjected to histological analysis using H&E staining. Arrows indicate the wound area.

bacterial small non-coding RNAs (sRNAs) include various species, with transfer RNAs (tRNAs) being particularly abundant and functionally relevant [73, 74]. Studies have shown that bacterial tRNA fragments (tRFs) can be transferred to mammalian cells, where they can modulate gene expression [74, 75]. For instance, tRFs from *E. coli* were found to be transferred via EVs to human cells, promoting MAP3K4 expression [76]. However, the function of full-length bacterial tRNA (over 75 bp) delivered via EVs to eukaryotic cells is less understood. A comparison between bacterial and mammalian RNA has shown that bacterial RNA effectively activates TLRs, specifically TLR3, TLR7, and TLR8, which are typically less responsive to mammalian cytosolic RNA [77]. *S. aureus* EV-derived RNA and DNA can function as ligands for intracellular receptor activation; meanwhile, dynamin-dependent endocytosis is strongly implicated in EV-mediated signaling to modulate the host immune response via endosomal TLR3 activation [32]. These findings highlight the role of bacterial nucleic acids in modulating immune responses and healing processes via extracellular trafficking.

The high abundance of tRNAs in Sm EVs, as demonstrated in this study, raises important questions about their selective packaging. One possibility is that tRNAs are preferentially enriched due to their structural stability [78]. Alternatively, stress-induced responses in *S. mutans* may influence EV cargo composition, leading to an enrichment of tRNAs that participate in host-microbe interactions [60]. Given that bacterial EVs are known to carry regulatory RNAs capable of modulating host immune pathways [79], tRNAs may serve key mediators in this interkingdom communication. Indeed, Tsatsaronis et al. emphasized the critical role of EVs as vehicles for microbial RNAs that engage host immune receptors and contribute to shaping microbial communities and host–microbe interactions [80]. Further studies need to be explored systematically whether other abundant sRNAs in Sm EVs also contribute to specific biological effects. In this study, we demonstrated the effects of Sm EVs on skin wound healing. Our results showed that Sm EVs promoted epithelial cell proliferation and migration in primary oral mucosal organoids. Consistent with these findings, H&E staining revealed that Sm EV treatment significantly enhanced epithelial regeneration in a mouse dorsal skin wound model (Fig. 2). Functionally, tRNA variants within the Sm EVs mediate this wound healing effect by stimulating host TLR3 (Fig. 3), which promotes cell proliferation and migration. To validate these findings, we synthesized an oligomer with the same sequence as the most abundant tRNA variants found in Sm EVs and used Ec EVs (which lack inherent wound healing properties) as a carrier to deliver the Sm EV tRNA oligomers into the skin (Fig. 8). However, in TLR3 KO mice, neither Sm EV nor Ec EV–Oligo 1 treatment accelerated wound healing (Fig. S10), suggesting that TLR3 plays a critical role in the wound healing effects driven by Sm EVs and their tRNA cargo. TLR3 is a vital pattern recognition receptors involved in innate and adaptive responses to tissue injury, recognizing double-stranded RNA (dsRNA) from sources like viruses or apoptotic cells [81]. Previous studies have shown that skin healing is impaired in TLR3-deficient mice, with reduced chemokine expression and myeloid cell recruitment [82]. Furthermore, TLR3 activation by its agonist enhanced skin wound healing by recruiting neutrophils and macrophages [83]. These findings, combined with our data, suggest that activating TLR3 with bacterial EVs [80], such as those from Sm EVs, could be a promising therapeutic strategy for wound healing. Our study also confirmed that Sm EVs deliver RNA cargo to endosomes, where TLR3 is primarily located. This supports the hypothesis that microbial RNAs interact with endosomal TLRs, distinct from host RNAs. Microbial nucleic acids are typically released into endosomes after immune cells, such as neutrophils and macrophages, phagocytose the microbes, distinguishing them from host RNAs [84]. Furthermore, EGFR binds to dsRNA-activated TLR3, triggering downstream signaling pathways that promote cell growth [85, 86]. In our study, Sm EVs promoted epithelial cell proliferation and migration via the EGFR (Fig. 4), further supporting a link between TLR3 activation and wound healing. Interestingly, despite the association of *S. mutans* and EGFR activation with OSCC progression [87], Sm EVs did not affect the proliferation or migration of OSCC. This suggests that the proliferative and migratory effects of Sm EVs are limited to normal mucosal cells and do not extend to cancerous cell growth.

While this study suggests that tRNA variants within bacterial EVs accelerate wound healing by promoting eukaryotic cell proliferation and migration, several limitations remain. One such limitation is that rodents primarily rely on wound contraction, which differs from the re-epithelialization process predominant in human wound healing. To compensate for this limitation, we performed histological analyses and observed more pronounced epithelial proliferation and regeneration in the wound tissues treated with Sm EVs or Ec EVs carrying Oligo 1,compared to the control group (Figs. 2B and 8C). In further studies, we aim to conduct more advanced investigations using stented wound models, with the ultimate goal of developing Sm EV- or tRNA-based therapeutic strategies for skin wound healing. Additionally, subsequent investigations are needed to delineate the specific contributions of EV-associated lipids, proteins, and RNA species, as other components may also influence the observed effects. In particular, identifying the specific RNA molecules responsible for the observed

effects—and determining whether these effects are governed by their sequence, secondary structure, or other physicochemical properties—will be essential. To better understand the specificity of *S. mutans*-derived EVs, we compared their effects with those of EVs from other oral streptococcal species. Notably, *S. salivarius* EVs exhibited similar wound-healing properties, whereas EVs from *S. gordonii* and *S. mitis* did not (data not shown), suggesting that *S. mutans* and *S. salivarius* EVs may contain species-specific cargo that enhances cellular activity. Ongoing work is focused on characterizing these EVs—particularly their sRNA cargo—to elucidate the molecular basis of this species-dependent activity. Additionally, while we employed Ec EVs as a delivery platform in this study, other RNA delivery mechanisms may also be explored in the future. A deeper understanding of the mechanisms by which microbial RNAs are packaged, released, and sensed by host receptors will provide valuable insights into host-microbe interactions and inform the development of next-generation EV-based therapeutics.

We acknowledge the importance of understanding the metabolism and clearance pathways of bacterial EVs *in vivo*. Previous studies have reported that bacterial EVs are rapidly cleared from circulation, primarily via hepatic and renal pathways, with a half-life of ≤ 30 min and complete clearance within 6 h [14, 15]. Although we did not assess the pharmacokinetics of Sm EVs in this study, future investigations will focus on tracking EV distribution, uptake, and clearance to better elucidate their systemic fate. In addition, understanding which specific cell types internalize Sm EVs will be essential to clarify their *in vivo* function and therapeutic effects. Further research is also needed to elucidate their biological activity and potential roles in modulating immune responses during wound healing. In supporting of this, our IHC analysis of wound tissues revealed increased recruitment of $CD3^+$ T cells, indicative of early immune activation, in both the Sm EV- and Ec EV–Oligo 1-treated groups (Fig. S11). Moreover, CD45 staining, which marks leukocytes, was more prominent in the granulation tissue of these treated wounds (Fig. S11), suggesting enhanced immune cell infiltration and active remodeling in the healing process.

While this study highlights the therapeutic potential of Sm EVs in wound healing, several translational challenges must be addressed. Large-scale production of EVs with consistent yield and bioactivity is a major hurdle, as current isolation methods are not easily scalable [88]. Additionally, EV stability during storage and transport remains a concern, as they are prone to aggregation, degradation, and functional loss under suboptimal conditions, potentially compromising therapeutic efficacy [89]. The mode of administration is also an important consideration. Although systemic injection is commonly employed in exosome-based therapies, Sm EVs may be more suitable for topical delivery—such as incorporation into hydrogel formulations—as this approach can enhance local retention at the wound site while minimizing systemic exposure [90, 91]. Moreover, regulatory approval will require rigorous quality control and safety assessments [85]. Given that *S. mutans* is a common commensal bacterium, the safety profile of Sm EVs is expected to be relatively favorable, with a low risk of adverse effects. Nevertheless, comprehensive studies are needed to evaluate their immunogenicity and long-term safety in clinical applications [92]. Addressing these gaps will deepen our understanding of the role of microbial EVs and their RNAs in wound healing and immune modulation. This knowledge could ultimately inform the development of more targeted and effective EV- and RNA-based therapeutic strategies for treating wounds and other related diseases.

Conclusions

This study demonstrates that *Streptococcus mutans*-derived extracellular vesicles (Sm EVs) promote epithelial proliferation and wound healing through a TLR3-dependent mechanism mediated by tRNA cargo, particularly a tRNA-Met variant. Our findings suggest that commensal bacterial EVs and their RNA cargo represent promising therapeutic tools for skin wound healing. Further characterization of EV components will be essential for translating these findings into clinical applications.

Supplementary Information

The online version contains supplementary material available at https://doi.org/10.1186/s12951-025-03410-1.

Supplementary Material 1

Author contributions

O.S.Y., L.H.J., C.S.Y. and H.S.H wrote the main manuscript. O.S.Y., L.H.J., L.K.Y., H.S.H., H.D.R. and K.D.Y. prepared Figs. 1, 3, 4 and 6. K.D.K., K.J.W., and C.S.Y. prepared Figs. 2 and 8. H.S.H., O.S.Y. L.K.Y., K.D.Y. and K.T.L. prepared Figs. 5 and 7. All authors reviewed the manuscript.

Funding

This work was supported by the Basic Science Research Program through a grant from the National Research Foundation (NRF) of Korea funded by the Ministry of Education, Science and Technology (2022R1A2C2006728, 2021R1A2C1004512), and in part by the ICT & Future Planning (2021R1A2C4002660).

Data availability

The total RNA sequencing data for Sm EVs have been deposited in Bioproject: PRJNA1168705 (SRR30883724).

Declarations

Ethics approval and consent to participate

Human tissue specimens were used with approval from the Institutional Research Ethics Committee of Kyungpook National University Hospital (KNUH 2021-03-002, 2023-12-03-00) after receiving written informed consent from the patients and in adherence with the principles of the Declaration of Helsinki. All experimental protocols with mice followed the ARRIVE guidelines

(Animal Research: Reporting of In Vivo Experiments) and were approved by the Animal Ethics Committee of Kyungpook National University (2023-0241-2).

Consent for publication
All authors have approved the manuscript and agree for the submission.

Competing interests
The authors declare no competing interests.

Author details
[1]Department of Microbiology and Immunology, School of Dentistry, Kyungpook National University, Daegu, South Korea
[2]Department of Dermatology, School of Medicine, Kyungpook National University, Daegu, South Korea
[3]Department of Oral and Maxillofacial Surgery, School of Dentistry, Kyungpook National University, Daegu, South Korea

Received: 8 January 2025 / Accepted: 19 April 2025
Published online: 28 April 2025

References

1. Kolenbrander PE, Andersen RN, Blehert DS, Egland PG, Foster JS, Palmer RJ Jr. Communication among oral bacteria. Microbiol Mol Biol Rev. 2002;66:486–505. table of contents.
2. Deo PN, Deshmukh R. Oral microbiome: unveiling the fundamentals. J Oral Maxillofac Pathol. 2019;23:122–28. https://www.ncbi.nlm.nih.gov/pubmed/31110428.
3. Krishnan K, Chen T, Paster BJ. A practical guide to the oral Microbiome and its relation to health and disease. Oral Dis. 2017;23:276–86. https://www.ncbi.nlm.nih.gov/pubmed/27219464.
4. Liu Y, Defourny KAY, Smid EJ, Abee T. Gram-Positive bacterial extracellular vesicles and their impact on health and disease. Front Microbiol. 2018;9. https://doi.org/10.3389/fmicb.2018.01502. https://www.frontiersin.org/articles/.
5. Gallo RL, Nakatsuji T. Microbial symbiosis with the innate immune defense system of the skin. J Invest Dermatol. 2011;131:1974–80. https://www.ncbi.nlm.nih.gov/pubmed/21697881.
6. Kong HH. Skin microbiome: genomics-based insights into the diversity and role of skin microbes. Trends Mol Med. 2011;17:320–8. https://www.ncbi.nlm.nih.gov/pubmed/21376666.
7. Belkaid Y, Segre JA. Dialogue between skin microbiota and immunity. Science. 2014;346:954–9. https://www.ncbi.nlm.nih.gov/pubmed/25414304.
8. Lai Y, Di Nardo A, Nakatsuji T, Leichtle A, Yang Y, Cogen AL, Wu ZR, Hooper LV, Schmidt RR, von Aulock S, et al. Commensal bacteria regulate Toll-like receptor 3-dependent inflammation after skin injury. Nat Med. 2009;15:1377–82. https://www.ncbi.nlm.nih.gov/pubmed/19966777.
9. Linehan JL, Harrison OJ, Han SJ, Byrd AL, Vujkovic-Cvijin I, Villarino AV, Sen SK, Shaik J, Smelkinson M, Tamoutounour S, et al. Non-classical immunity controls microbiota impact on skin immunity and tissue repair. Cell. 2018;172:784–e9618. https://www.ncbi.nlm.nih.gov/pubmed/29358051.
10. Zheng D, Liwinski T, Elinav E. Interaction between microbiota and immunity in health and disease. Cell Res. 2020;30:492–506. https://www.ncbi.nlm.nih.gov/pubmed/32433595.
11. De Ryck T, Vanlancker E, Grootaert C, Roman BI, De Coen LM, Vandenberghe I, Stevens CV, Bracke M, Van de Wiele T, Vanhoecke B. Microbial Inhibition of oral epithelial wound recovery: potential role for quorum sensing molecules? AMB Express. 2015;5:27. https://www.ncbi.nlm.nih.gov/pubmed/25995981.
12. Hong SW, Baik JE, Kang SS, Yun CH, Seo DG, Han SH. Lipoteichoic acid of Streptococcus mutans interacts with Toll-like receptor 2 through the lipid moiety for induction of inflammatory mediators in murine macrophages. Mol Immunol. 2014;57:284–91. https://www.ncbi.nlm.nih.gov/pubmed/24216318.
13. Fournier BP, Ferre FC, Couty L, Lataillade JJ, Gourven M, Naveau A, Coulomb B, Lafont A, Gogly B. Multipotent progenitor cells in gingival connective tissue. Tissue Eng Part A. 2010;16:2891–9. https://www.ncbi.nlm.nih.gov/pubmed/20412029.
14. Wang F, Yu M, Yan X, Wen Y, Zeng Q, Yue W, Yang P, Pei X. Gingiva-derived mesenchymal stem cell-mediated therapeutic approach for bone tissue regeneration. Stem Cells Dev. 2011;20:2093–102. https://www.ncbi.nlm.nih.gov/pubmed/21361847.
15. Widera D, Zander C, Heidbreder M, Kasperek Y, Noll T, Seitz O, Saldamli B, Sudhoff H, Sader R, Kaltschmidt C, Kaltschmidt B. Adult palatum as a novel source of neural crest-related stem cells. Stem Cells. 2009;27:1899–910. https://www.ncbi.nlm.nih.gov/pubmed/19544446.
16. Waasdorp M, Krom BP, Bikker FJ, van Zuijlen PPM, Niessen FB, Gibbs S. The bigger picture: why oral mucosa heals better than skin. Biomolecules 2021;11. https://www.ncbi.nlm.nih.gov/pubmed/34439831
17. Rodrigues Neves C, Buskermolen J, Roffel S, Waaijman T, Thon M, Veerman E, Gibbs S. Human saliva stimulates skin and oral wound healing in vitro. J Tissue Eng Regen Med. 2019;13:1079–92. https://www.ncbi.nlm.nih.gov/pubmed/30968584.
18. Brand HS, Ligtenberg AJ, Veerman EC. Saliva and wound healing. Monogr Oral Sci. 2014;24:52–60. https://www.ncbi.nlm.nih.gov/pubmed/24862594.
19. Matee MI, Simon E. Saliva and salivary gland alterations in HIV infection: a review. Afr Dent J. 1995;9:25–9. https://www.ncbi.nlm.nih.gov/pubmed/9590897.
20. Marynka-Kalmani K, Treves S, Yafee M, Rachima H, Gafni Y, Cohen MA, Pitaru S. The lamina propria of adult human oral mucosa harbors a novel stem cell population. Stem Cells. 2010;28:984–95. https://www.ncbi.nlm.nih.gov/pubmed/20474080.
21. Michalczyk ERS, Jones AR, Coulter RM, Goudy WH. Changes in the Microbiome during oral wound healing. Dentistry Rev. 2022;2:100040–48.
22. Nahui Palomino RA, Vanpouille C, Costantini PE, Margolis L. Microbiota-host communications: bacterial extracellular vesicles as a common Language. PLoS Pathog. 2021;17:e1009508. https://www.ncbi.nlm.nih.gov/pubmed/33984071.
23. Zou C, Zhang Y, Liu H, Wu Y, Zhou X. Extracellular vesicles: recent insights into the interaction between host and pathogenic Bacteria. Front Immunol. 2022;13:840550. https://www.ncbi.nlm.nih.gov/pubmed/35693784.
24. Schwechheimer C, Kuehn MJ. Outer-membrane vesicles from Gram-negative bacteria: biogenesis and functions. Nat Rev Microbiol. 2015;13:605–19. https://www.ncbi.nlm.nih.gov/pubmed/26373371.
25. Wang X, Thompson CD, Weidenmaier C, Lee JC. Release of Staphylococcus aureus extracellular vesicles and their application as a vaccine platform. Nat Commun. 2018;9:1379. https://www.ncbi.nlm.nih.gov/pubmed/29643357.
26. Wu R, Cui G, Cao Y, Zhao W, Lin H. Streptococcus Mutans membrane vesicles enhance Candida albicans pathogenicity and carbohydrate metabolism. Front Cell Infect Microbiol. 2022;12:940602. https://www.ncbi.nlm.nih.gov/pubmed/35959374.
27. Wen ZT, Jorgensen AN, Huang X, Ellepola K, Chapman L, Wu H, Jeannine Brady L. Multiple factors are involved in regulation of extracellular membrane vesicle biogenesis in Streptococcus mutans. Mol Oral Microbiol. 2021;36:12–24. https://www.ncbi.nlm.nih.gov/pubmed/33040492.
28. Liao S, Klein MI, Heim KP, Fan Y, Bitoun JP, Ahn SJ, Burne RA, Koo H, Brady LJ, Wen ZT. Streptococcus mutans extracellular DNA is upregulated during growth in biofilms, actively released via membrane vesicles, and influenced by components of the protein secretion machinery. J Bacteriol. 2014;196:2355–66. https://www.ncbi.nlm.nih.gov/pubmed/24748612.
29. Nakamura T, Iwabuchi Y, Hirayama S, Narisawa N, Takenaga F, Nakao R, Senpuku H. Roles of membrane vesicles from Streptococcus mutans for the induction of antibodies to glucosyltransferase in mucosal immunity. Microb Pathog. 2020;149:104260. https://www.ncbi.nlm.nih.gov/pubmed/32554054.
30. Eberle F, Sirin M, Binder M, Dalpke AH. Bacterial RNA is recognized by different sets of immunoreceptors. Eur J Immunol. 2009;39:2537–47. https://www.ncbi.nlm.nih.gov/pubmed/19662634.
31. Tan X, Sun L, Chen J, Chen ZJ. Detection of microbial infections through innate immune sensing of nucleic acids. Annu Rev Microbiol. 2018;72:447–78. https://www.ncbi.nlm.nih.gov/pubmed/30200854.
32. Rodriguez BV, Kuehn MJ. Staphylococcus aureus secretes Immunomodulatory RNA and DNA via membrane vesicles. Sci Rep. 2020;10:18293. https://www.ncbi.nlm.nih.gov/pubmed/33106559.
33. Lee MS, Kim YJ. Signaling pathways downstream of pattern-recognition receptors and their cross talk. Annu Rev Biochem. 2007;76:447–80. https://www.ncbi.nlm.nih.gov/pubmed/17328678.
34. Nellimarla S, Mossman KL. Extracellular DsRNA: its function and mechanism of cellular uptake. J Interferon Cytokine Res. 2014;34:419–26. https://www.ncbi.nlm.nih.gov/pubmed/24905198.
35. Wang Y, Swiecki M, McCartney SA, Colonna M. DsRNA sensors and plasmacytoid dendritic cells in host defense and autoimmunity. Immunol Rev. 2011;243:74–90. https://www.ncbi.nlm.nih.gov/pubmed/21884168.

36. Duan T, Du Y, Xing C, Wang HY, Wang RF. Toll-Like receptor signaling and its role in Cell-Mediated immunity. Front Immunol. 2022;13:812774. https://www.ncbi.nlm.nih.gov/pubmed/35309296.
37. Zhao R, Zhang J, Wang Y, Jin J, Zhou H, Chen J, Su SB. Activation of Toll-like receptor 3 promotes pathological corneal neovascularization by enhancement of SDF-1-mediated endothelial progenitor cell recruitment. Exp Eye Res. 2019;178:177–85. https://www.ncbi.nlm.nih.gov/pubmed/30321512.
38. Landen NX, Li D, Stahle M. Transition from inflammation to proliferation: a critical step during wound healing. Cell Mol Life Sci. 2016;73:3861–85. https://www.ncbi.nlm.nih.gov/pubmed/27180275.
39. Jockel S, Nees G, Sommer R, Zhao Y, Cherkasov D, Hori H, Ehm G, Schnare M, Nain M, Kaufmann A, Bauer S. The 2'-O-methylation status of a single Guanosine controls transfer RNA-mediated Toll-like receptor 7 activation or Inhibition. J Exp Med. 2012;209:235–41. https://www.ncbi.nlm.nih.gov/pubmed/22312111.
40. Johnson TR, Gomez BI, McIntyre MK, Dubick MA, Christy RJ, Nicholson SE, Burmeister DM. The cutaneous Microbiome and wounds: new molecular targets to promote wound healing. Int J Mol Sci 2018;19. https://www.ncbi.nlm.nih.gov/pubmed/30208569
41. Joshi B, Singh B, Nadeem A, Askarian F, Wai SN, Johannessen M, Hegstad K. Transcriptome profiling of Staphylococcus aureus associated extracellular vesicles reveals presence of small RNA-Cargo. Front Mol Biosci. 2020;7:566207. https://www.ncbi.nlm.nih.gov/pubmed/33521050.
42. Kim SI, Ha JY, Choi SY, Hong SH, Lee HJ. Use of bacterial extracellular vesicles for gene delivery to host cells. Biomolecules 2022;12. https://www.ncbi.nlm.nih.gov/pubmed/36139009
43. Diaz-Garrido N, Bonnin S, Riera M, Gimenez R, Badia J, Baldoma L. Transcriptomic MicroRNA profiling of dendritic cells in response to gut Microbiota-Secreted vesicles. Cells 2020;9. https://www.ncbi.nlm.nih.gov/pubmed/32585977
44. Driehuis E, Kolders S, Spelier S, Lohmussaar K, Willems SM, Devriese LA, de Bree R, de Ruiter EJ, Korving J, Begthel H, et al. Oral mucosal organoids as a potential platform for personalized Cancer therapy. Cancer Discov. 2019;9:852–71. https://www.ncbi.nlm.nih.gov/pubmed/31053628.
45. Driehuis E, Kretzschmar K, Clevers H. Establishment of patient-derived cancer organoids for drug-screening applications. Nat Protoc. 2020;15:3380–409. https://www.ncbi.nlm.nih.gov/pubmed/32929210.
46. Oh SY, Kim J, Lee KY, Lee HJ, Kwon TG, Kim JW, Lee ST, Kim DG, Choi SY, Hong SH. Chromatin remodeling-driven autophagy activation induces cisplatin resistance in oral squamous cell carcinoma. Cell Death Dis. 2024;15:589. https://www.ncbi.nlm.nih.gov/pubmed/39138148.
47. Fan B, Wang T, Bian L, Jian Z, Wang DD, Li F, Wu F, Bai T, Zhang G, Muller N, et al. Topical application of Tat-Rac1 promotes cutaneous wound healing in normal and diabetic mice. Int J Biol Sci. 2018;14:1163–74. https://www.ncbi.nlm.nih.gov/pubmed/30123066.
48. Rowland MB, Moore PE, Bui C, Correll RN. Assessing wound closure in mice using skin-punch biopsy. STAR Protoc. 2023;4:101989. https://www.ncbi.nlm.nih.gov/pubmed/36602903.
49. Chakrabarti J, Koh V, So JBY, Yong WP, Zavros Y. A preclinical Human-Derived autologous gastric Cancer organoid/immune cell Co-Culture model to predict the efficacy of targeted therapies. J Vis Exp 2021. https://www.ncbi.nlm.nih.gov/pubmed/34309588
50. Zahm JM, Kaplan H, Hérard AL, Doriot F, Pierrot D, Somelette P, Puchelle E. Cell migration and proliferation during the in vitro wound repair of the respiratory epithelium. Cell Motil Cytoskeleton. 1997;37:33–43.
51. Puri S, Sun M, Mutoji KN, Gesteira TF, Coulson-Thomas VJ. Epithelial cell migration and proliferation patterns during initial wound closure in normal mice and an experimental model of limbal stem cell deficiency. Invest Ophthalmol Vis Sci. 2020;61:27.
52. Alexander PB, Yuan L, Yang P, Sun T, Chen R, Xiang H, Chen J, Wu H, Radiloff DR, Wang X-F. EGF promotes mammalian cell growth by suppressing cellular senescence. Cell Res. 2015;25:135–38. https://doi.org/10.1038/cr.2014.141.
53. Sturla LM, Amorino G, Alexander MS, Mikkelsen RB, Valerie K, Schmidt-Ullrichr RK. Requirement of Tyr-992 and Tyr-1173 in phosphorylation of the epidermal growth factor receptor by ionizing radiation and modulation by SHP2. J Biol Chem. 2005;280:14597–604. https://www.ncbi.nlm.nih.gov/pubmed/15708852.
54. Sorkin A, Goh LK. Endocytosis and intracellular trafficking of ErbBs. Exp Cell Res. 2008;314:3093–106. https://www.ncbi.nlm.nih.gov/pubmed/18793634.
55. Chen R, Jin G, Li W, McIntyre TM. Epidermal growth factor (EGF) autocrine activation of human platelets promotes EGF Receptor-Dependent oral squamous cell carcinoma invasion, migration, and epithelial mesenchymal transition. J Immunol. 2018;201:2154–64. https://www.ncbi.nlm.nih.gov/pubmed/30150285.
56. Katoh K. FAK-Dependent Cell Motility and Cell Elongation. In *Cells*, vol. 9; 2020.
57. Deakin NO, Turner CE. Paxillin comes of age. J Cell Sci. 2008;121:2435–44. https://www.ncbi.nlm.nih.gov/pubmed/18650496.
58. Hu YL, Lu S, Szeto KW, Sun J, Wang Y, Lasheras JC, Chien S. FAK and paxillin dynamics at focal adhesions in the protrusions of migrating cells. Sci Rep. 2014;4:6024. https://www.ncbi.nlm.nih.gov/pubmed/25113375.
59. Gandek TB, van der Koog L, Nagelkerke A. A comparison of cellular uptake mechanisms, delivery efficacy, and intracellular fate between liposomes and extracellular vesicles. Adv Healthc Mater. 2023;12:e2300319. https://www.ncbi.nlm.nih.gov/pubmed/37384827.
60. Hosseini-Giv N, Basas A, Hicks C, El-Omar E, El-Assaad F, Hosseini-Beheshti E. Bacterial extracellular vesicles and their novel therapeutic applications in health and cancer. Front Cell Infect Microbiol. 2022;12:962216. https://www.ncbi.nlm.nih.gov/pubmed/36439225.
61. Liu H, Zhang Q, Wang S, Weng W, Jing Y, Su J. Bacterial extracellular vesicles as bioactive nanocarriers for drug delivery: advances and perspectives. Bioact Mater. 2022;14:169–81. https://www.ncbi.nlm.nih.gov/pubmed/35310361.
62. Byrd KM, Piehl NC, Patel JH, Huh WJ, Sequeira I, Lough KJ, Wagner BL, Marangoni P, Watt FM, Klein OD, et al. Heterogeneity within stratified epithelial stem cell populations maintains the oral mucosa in response to physiological stress. Cell Stem Cell. 2019;25:814–e296. https://www.ncbi.nlm.nih.gov/pubmed/31809739.
63. Kuperman S, Efraty R, Arie I, Rahmanov A, Rahmanov Gavrielov M, Noff M, Fishel R, Pitaru S. Examination of the therapeutic potential of mouse oral mucosa stem cells in a Wound-Healing diabetic mice model. Int J Environ Res Public Health 2020;17. https://www.ncbi.nlm.nih.gov/pubmed/32640560
64. Guo J, Huang Z, Wang Q, Wang M, Ming Y, Chen W, Huang Y, Tang Z, Huang M, Liu H, Jia B. Opportunities and challenges of bacterial extracellular vesicles in regenerative medicine. J Nanobiotechnol. 2025;23:4. https://www.ncbi.nlm.nih.gov/pubmed/39754127.
65. Abdullah Z, Schlee M, Roth S, Mraheil MA, Barchet W, Bottcher J, Hain T, Geiger S, Hayakawa Y, Fritz JH, et al. RIG-I detects infection with live Listeria by sensing secreted bacterial nucleic acids. EMBO J. 2012;31:4153–64. https://www.ncbi.nlm.nih.gov/pubmed/23064150.
66. Rodriguez-Rodrigues N, Castillo LA, Landoni VI, Martire-Greco D, Milillo MA, Barrionuevo P, Fernandez GC. Prokaryotic RNA associated to bacterial viability induces polymorphonuclear neutrophil activation. Front Cell Infect Microbiol. 2017;7:306. https://www.ncbi.nlm.nih.gov/pubmed/28730145.
67. Kamm RC, Smith AG. Ribonuclease activity in human plasma. Clin Biochem. 1972;5:198–200. https://www.ncbi.nlm.nih.gov/pubmed/4674387.
68. Blenkiron C, Simonov D, Muthukaruppan A, Tsai P, Dauros P, Green S, Hong J, Print CG, Swift S, Phillips AR. Uropathogenic Escherichia coli releases extracellular vesicles that are associated with RNA. PLoS ONE. 2016;11:e0160440. https://www.ncbi.nlm.nih.gov/pubmed/27500956.
69. Resch U, Tsatsaronis JA, Le Rhun A, Stubiger G, Rohde M, Kasvandik S, Holzmeister S, Tinnefeld P, Wai SN, Charpentier E. A Two-Component regulatory system impacts extracellular Membrane-Derived vesicle production in group A Streptococcus. mBio 2016;7. https://www.ncbi.nlm.nih.gov/pubmed/27803183
70. Wagner EGH, Romby P. Small RNAs in bacteria and Archaea: who they are, what they do, and how they do it. Adv Genet. 2015;90:133–208. https://www.ncbi.nlm.nih.gov/pubmed/26296935.
71. Carrier MC, Lalaouna D, Masse E. Broadening the definition of bacterial small RNAs: characteristics and mechanisms of action. Annu Rev Microbiol. 2018;72:141–61. https://www.ncbi.nlm.nih.gov/pubmed/30200848.
72. Storz G, Vogel J, Wassarman KM. Regulation by small RNAs in bacteria: expanding frontiers. Mol Cell. 2011;43:880–91. https://www.ncbi.nlm.nih.gov/pubmed/21925377.
73. Tosar JP, Cayota A. Extracellular tRNAs and tRNA-derived fragments. RNA Biol. 2020;17:1149–67. https://www.ncbi.nlm.nih.gov/pubmed/32070197.
74. Lecrivain AL, Beckmann BM. Bacterial RNA in extracellular vesicles: A new regulator of host-pathogen interactions? Biochim Biophys Acta Gene Regul Mech. 2020;1863:194519. https://www.ncbi.nlm.nih.gov/pubmed/32142907.
75. Li Z, Stanton BA. Transfer RNA-Derived fragments, the underappreciated regulatory small RNAs in microbial pathogenesis. Front Microbiol. 2021;12:687632. https://www.ncbi.nlm.nih.gov/pubmed/34079534.
76. Diallo I, Ho J, Lambert M, Benmoussa A, Husseini Z, Lalaouna D, Masse E, Provost P. A tRNA-derived fragment present in E. coli OMVs regulates host cell

gene expression and proliferation. PLoS Pathog. 2022;18:e1010827. https://www.ncbi.nlm.nih.gov/pubmed/36108089.
77. Dalpke A, Helm M. RNA mediated Toll-like receptor stimulation in health and disease. RNA Biol. 2012;9:828–42. https://www.ncbi.nlm.nih.gov/pubmed/22617878.
78. Biedenbander T, de Jesus V, Schmidt-Dengler M, Helm M, Corzilius B, Furtig B. RNA modifications stabilize the tertiary structure of tRNAfMet by locally increasing conformational dynamics. Nucleic Acids Res. 2022;50:2334–49. https://www.ncbi.nlm.nih.gov/pubmed/35137185.
79. Diaz-Garrido N, Badia J, Baldoma L. Microbiota-derived extracellular vesicles in interkingdom communication in the gut. J Extracell Vesicles. 2021;10:e12161. https://www.ncbi.nlm.nih.gov/pubmed/34738337.
80. Tsatsaronis JA, Franch-Arroyo S, Resch U, Charpentier E. Extracellular vesicle RNA: A universal mediator of microbial communication?? Trends Microbiol. 2018;26:401–10. https://www.ncbi.nlm.nih.gov/pubmed/29548832.
81. Matsumoto M, Seya T. TLR3: interferon induction by double-stranded RNA including poly(I:C). Adv Drug Deliv Rev. 2008;60:805–12. https://www.ncbi.nlm.nih.gov/pubmed/18262679.
82. Lin Q, Fang D, Fang J, Ren X, Yang X, Wen F, Su SB. Impaired wound healing with defective expression of chemokines and recruitment of myeloid cells in TLR3-deficient mice. J Immunol. 2011;186:3710–7. https://www.ncbi.nlm.nih.gov/pubmed/21317384.
83. Lin Q, Wang L, Lin Y, Liu X, Ren X, Wen S, Du X, Lu T, Su SY, Yang X, et al. Toll-like receptor 3 ligand polyinosinic:polycytidylic acid promotes wound healing in human and murine skin. J Invest Dermatol. 2012;132:2085–92. https://www.ncbi.nlm.nih.gov/pubmed/22572822.
84. Minton K. Regulation of endosomal TLRs. Nat Rev Immunol. 2019;19:660–61. https://www.ncbi.nlm.nih.gov/pubmed/31562494.
85. Yamashita M, Chattopadhyay S, Fensterl V, Saikia P, Wetzel JL, Sen GC. Epidermal growth factor receptor is essential for Toll-like receptor 3 signaling. Sci Signal. 2012;5:ra50. https://www.ncbi.nlm.nih.gov/pubmed/22810896.
86. Xia W, Wei Y, Du Y, Liu J, Chang B, Yu Y-L, Huo L-F, Miller S, Hung M-C. Nuclear expression of epidermal growth factor receptor is a novel prognostic value in patients with ovarian cancer. Mol Carcinog. 2009;48:610–17. https://doi.org/10.1002/mc.20504.
87. Tsai MS, Chen YY, Chen WC, Chen MF. Streptococcus mutans promotes tumor progression in oral squamous cell carcinoma. J Cancer. 2022;13:3358–67. https://www.ncbi.nlm.nih.gov/pubmed/36186905.
88. Yamashita T, Takahashi Y, Takakura Y. Possibility of Exosome-Based therapeutics and challenges in production of exosomes eligible for therapeutic application. Biol Pharm Bull. 2018;41:835–42. https://www.ncbi.nlm.nih.gov/pubmed/29863072.
89. Bosch S, de Beaurepaire L, Allard M, Mosser M, Heichette C, Chretien D, Jegou D, Bach JM. Trehalose prevents aggregation of exosomes and Cryodamage. Sci Rep. 2016;6:36162. https://www.ncbi.nlm.nih.gov/pubmed/27824088.
90. Ju Y, Hu Y, Yang P, Xie X, Fang B. Extracellular vesicle-loaded hydrogels for tissue repair and regeneration. Mater Today Bio. 2023;18:100522. https://www.ncbi.nlm.nih.gov/pubmed/36593913.
91. Palakurthi SS, Shah B, Kapre S, Charbe N, Immanuel S, Pasham S, Thalla M, Jain A, Palakurthi S. A comprehensive review of challenges and advances in exosome-based drug delivery systems. Nanoscale Adv. 2024;6:5803–26. https://www.ncbi.nlm.nih.gov/pubmed/39484149.
92. Herrmann IK, Wood MJA, Fuhrmann G. Extracellular vesicles as a next-generation drug delivery platform. Nat Nanotechnol. 2021;16:748–59. https://www.ncbi.nlm.nih.gov/pubmed/34211166.

Publisher's note